CIAMTIS

U.S. DOT Region 3 University Transportation Center

Time-based Modeling of Concrete Bridge Deck Deterioration Using Probabilistic Models

February 15, 2021

Prepared by:

S.I. Guler, A. Radlinska, M. Lu, J. Hydock

The Pennsylvania State University

r3utc.psu.edu

PennState College of Engineering

LARSON TRANSPORTATION INSTITUTE

DISCLAIMER

Technical Report Documentation Page

1. Report No.	2. Government Accession No.	3. Recipient's Catalog No.
CIAM-UTC-REG10		

4. Title and Subtitle	5. Report Date
Time-Based Modeling of Concrete Bridge Deck Deterioration Using Probabilistic Models	February 15, 2021
	6. Performing Organization Code
7. Author(s)	**8. Performing Organization Report No.**
Guler, S.I., https://orcid.org/0000-0001-6255-3135 Radlinska, A., https://orcid.org/0000-0002-7977-4927 Lu, M., and Hydock, J.	LTI 2021-06
9. Performing Organization Name and Address	**10. Work Unit No. (TRAIS)**
Department of Civil and Environmental Engineering Pennsylvania State University 215 Sackett Building University Park, PA 16802	**11. Contract or Grant No.** 69A3551847103
12. Sponsoring Agency Name and Address	**13. Type of Report and Period Covered**
U.S. Department of Transportation Research and Innovative Technology Administration 3rd Fl, East Bldg E33-461 1200 New Jersey Ave, SE Washington, DC 20590	Final Report 03/01/2019 – 08/31/2021 **14. Sponsoring Agency Code**

15. Supplementary Notes

Work funded through The Pennsylvania State University through the University Transportation Center Grant Agreement, Grant No. 69A3551847103.

16. Abstract

This research developed a robust, self-learning, probabilistic model to predict the service life of concrete bridge decks and subsequently other infrastructure components. The model originated from the existing performance data for 22,000 bridge decks in the State of Pennsylvania and utilized advanced statistical tools, including Bayesian probabilistic networks. The newly developed tool can allow state departments of transportation to: (1) accurately predict the lifetime of concrete bridge decks, and (2) establish more efficient and accurate management decisions, resulting in increased longevity of the nation's infrastructure.

17. Key Words	18. Distribution Statement
Infrastructure management, bridge deck deterioration, Bayesian optimzation	No restrictions. This document is available from the National Technical Information Service, Springfield, VA 22161

19. Security Classif. (of this report)	20. Security Classif. (of this page)	21. No. of Pages	22. Price
Unclassified	Unclassified	45	

Form DOT F 1700.7 **(8-72) Reproduction of completed page authorized**

Table of Contents

1. Introduction **1**
Background 1
Objectives 1
Data and Data Structures 1

2. Background **3**

3. Methodology **5**
Introduction 5
Weibull Deterioration Model 5
Accelerated-failure Time Model 6

4. Data Processing and Exploration **13**
Introduction 13
Rebar Type 16
Span Number 18
Surface Type 19
Year Constructed 20

5. Findings of the Weibull Deterioration Model **23**

6. Findings of the Accelerated-failure Time Model **26**
Choosing the Dependent Variable 26
Verifying the Choice of Generalized Gamma Distribution 28
Verifying the Accuracy of the MCMC Methodology 28
Estimation of the Full Model 30

7. Recommendations **38**

References **39**

List of Figures

Figure 1. Demolition of a bridge in Pennsylvania. The state has the highest number of structurally deficient bridges 1
Figure 2. Likelihood distribution of the generalized gamma distribution..... 10
Figure 3. Transformed likelihood distribution of the generalized gamma function 12
Figure 4. Distribution of complete and right-censored data for different CRs 15
Figure 5. Distribution for rebar type by condition rating of: (a) sojourn time, (b) number of bridges, (c) average daily truck traffic, and (d) cumulative truck traffic 17
Figure 6. Distribtuion for span type by condition rating of: (a) sojourn time, (b) number of bridges, (c) average daily truck traffic and (d) cumulative truck traffic 18
Figure 7. Distribution for surface type by condition rating of: (a) sojourn time, (b) number of bridges, (c) average daily truck traffic and (d) cumulative truck traffic 19
Figure 8. Construction year of all bridges..... 20
Figure 9. Distributions for different construction years by condition rating of: (a) sojourn time, (b) number of bridges, (c) average daily truck traffic and (d) cumulative truck traffic 21
Figure 10. Estimated reliability curves of different distributions compared to the real deterioration pattern: (a) Weibull distribution, (b) exponential distribution, (c) log-normal distribution, (d) log-logistic distribution, (e) piecewise exponential distribution, and (f) generalized gamma distribution..... 22
Figure 11. Prediction of Weibull model for each condition rating 23
Figure 12. Sensitivity analysis of weights of different attributes..... 25
Figure 13. Deterioration pattern with time until change in CR as the independent variable 27
Figure 14. Deterioration pattern with CTT as the independent variable..... 27
Figure 15. Results of different distributions used to model bridge survival probability function 28
Figure 16. Comparison of estimation results of bared rebar type 29
Figure 17. Comparison of MCMC results and Kaplan-Meier estimation: (a) bare rebar, (b) galvanized rebar, (c) epoxy rebar, and (d) other rebar types (baseline) 29
Figure 18. Parameters of DISTRICT in each condition rating 33
Figure 19. Parameters of DEPT_MAIN_PHYSICAL_TYPE in each condition rating 33
Figure 20. Parameters of DEPT_MAIN_SPAN_INTERACTION in each condition rating..... 34
Figure 21. Parameters of DECK_REBAR_TYPE in each condition rating 35
Figure 22. Parameters of SPECIAL EVENTS in each condition rating..... 36
Figure 23. Bayesian updating results 37

List of Tables

Table 1. Attributes description and values distribution 14
Table 2. Statistic of sojourn times (in days) of bridge decks 15
Table 3. Model parameter estimation results of CR 7 24
Table 4. Combined prediction of deterioration probability of the bridge 24
Table 5. Confusion matrix of the predictive model 30
Table 6. Estimated parameters of the full model 31
Table 7. Dataset description..... 36

CHAPTER 1

Introduction

BACKGROUND

Accurate prediction of the performance of infrastructure components, including concrete bridge decks, is essential when determining the maintenance and repair actions to be performed on the element throughout its lifetime. By using accurate estimates, agency costs due to maintenance, repair and reconstruction, along with user costs, can all be minimized. Transportation agencies most often use discrete condition ratings (CRs) to assess the state of the bridge deck in order to simplify the decision-making and inspection procedures. For example, in Pennsylvania, decks are rated from 0 (worst) to 9 (best) based on performance criteria such as delamination, spalling, electrical potential, and chloride content (PennDOT, 2009). While recently completed research attempted to incorporate the extent of cracking into the rating system (Manafpour et al., 2016), more work is needed to develop accurate and reliable models predicting the lifecycle of bridge decks and other infrastructure systems.

Figure 1. Demolition of a bridge in Pennsylvania. The state has the highest number of structurally deficient bridges. [PennDOT 2009]

OBJECTIVES

The goal of the research was to develop a robust, self-learning, probabilistic model to predict the service life of concrete bridge decks and subsequently other infrastructure components. The model originates from the existing performance data for 22,000 bridge decks in the State of Pennsylvania and utilizes advanced statistical tools, including machine learning systems and Bayesian probabilistic networks. The newly developed tool will allow state departments of transportation to: (1) accurately predict the lifetime of concrete bridge decks and (2) establish more efficient and accurate management decisions, resulting in increased longevity of the nation's infrastructure.

DATA AND DATA STRUCTURES

The dataset analyzed in this work consists of biannual inspections of bridges across Pennsylvania obtained from the Pennsylvania Department of Transportation (PennDOT). Historical bridge deck condition ratings (CRs) along with attributes of the bridge structure obtained from the Bridge Management System (BMS2)

(PennDOT, 2009) were accessed for over 22,000 bridge decks inspected between 1985 and 2015. Condition ratings range from 0 to 9. Greater than or equal to a rating of 7 is considered "good," ratings of 5 and 6 are considered "fair," and ratings below 5 are considered "poor" in relation to their condition (PennDOT 2020, Pub 408).

CHAPTER 2

Background

Different approaches for modeling infrastructure deterioration exist in the literature, including linear regression (O'Leary et al., 2012; Zhang and Durango-Cohen, 2014), Markov chain models (Agrawal et al., 2010; Manafpour et al., 2018), and stochastic duration models (Agrawal et al., 2010; Cox and Matheson, 2014). Linear models assume that the future condition rating of a bridge deck is deterministic. In reality, the evolution of the condition of a bridge deck is considered to be a stochastic process due to the multiple stochastic factors that affect the rating (e.g., traffic and weather), which is captured by the latter two models. In general, probabilistic models are deemed more appropriate to model and predict the performance of concrete bridge decks to account for this stochasticity.

The Markov chain method is the most commonly used method for stochastic modeling of the deterioration process. This method aims at modeling the probability that the (discrete) condition of a bridge deck decreases; however, it assumes that the deterioration is independent of age, which is a significant limitation (Agrawal et al., 2010). Some improvements to the Markov chain approach have been proposed, such as the semi-Markov chain (Manafpour et al., 2018). The transition probabilities of semi-Markov chain models can be duration dependent, unlike Markov chain processes. However, both Markov chain and semi-Markov chain-based approaches still omit censored data, which are typically dominant in the dataset. Distribution-based duration models typically perform better at predicting deterioration, since time and right-censored data can also be incorporated in the models (Agrawal et al., 2010). While Weibull is the most popular distribution used for modeling infrastructure, other distributions can also be used within these distribution-based approaches. For example, the generalized gamma distribution has been used to model the survival from AIDS considering different therapies (Cox and Matheson, 2014) or to study the survival of firms (Kaniovski and Peneder, 2008).

Additionally, methods that rely solely on the data, such as machine learning methods, can be used to model infrastructure deterioration. One study compared five different kinds of data mining techniques for steel bridge superstructure deterioration: (1) logistic regression, (2) decision trees, (3) neural network, (4) gradient boosting, and (5) support vector machine. The results showed that logistic regression was able to obtain the highest prediction accuracy (Contreras-Nieto et al., 2018). Another study only focused on the backpropagation-multilayer perceptron (BP-MLP) neural network method for modeling bridge deterioration and obtained a prediction accuracy of 75.38% on the test dataset. However, that method was not able to incorporate censored data (Huang, 2010). A recent study designed an integrated deterioration approach that incorporates a time-based model, a state-based model with the Elman neural network (ENN), and a backward prediction model (BPM) for prediction of long-term bridge performance (Bu et al., 2015). Another study investigated the use of the recursive partitioning method to develop classification trees that predict National Bridge Inventory condition ratings from national bridge elements condition data (Bektas, 2017). However, the accuracy of these machine learning methods highly relies on the scale of the input dataset, and more problematically, the interpretation of the model parameters is a big challenge.

As new data become available, the complete reestimation of existing models can be computationally costly and drastically change the way the models need to be implemented. Bayesian theory provides a way to incorporate newly available data into the prediction model without having to rebuild the entire model. Bayesian theory assumes that an a-priori distribution for the parameters exists and updates these a-priori assumptions to derive posterior distributions of the parameters based on the available data. Several methods that use Bayesian inference to update the parameters of a prediction model have been proposed for models with a dependent variable that follows a normal distribution (Bayes and Branco, 2007; Belitser and Ghosal, 2003) or a log-normal distribution, which can better account for extreme values (Strauss et al., 2008; Enrique, 2006). A recent work utilized the Bayesian inference method for a Weibull distribution for the reliability analysis of satellites. In that method Beta distributions were used to estimate the parameters of the Weibull distribution, which could then be used as an a-priori distribution to update the parameters when new data become available (Yang et al., 2018). Similarly, another recent work used the Bayesian inference method for a generalized gamma distribution of reliability (de Pascoa et al., 2011). However, neither of these works incorporated covariates in the model, thus neither can be utilized to analyze the influence of external variables on the failure process.

CHAPTER 3

Methodology

INTRODUCTION

The goal of this project was to model the duration a bridge deck lasts in a given condition rating using a survival analysis that can better account for the variability in the inspection data and can self-update as new data become available. For these models, the time a bridge deck lasts in a given CR or cumulative truck traffic in a given CR is considered as the independent variable. These variables are modeled assuming they follow a generalized gamma distribution using an accelerated failure time model. The parameters of this model are estimated using Markov chain Monte Carlo (MCMC) models that can provide ranges of confidence for the results, and additionally, can be combined with Bayesian inference for updating the parameters as new data become available, without reestimating the entire model. The different steps of the methodology are discussed below.

WEIBULL DETERIORATION MODEL

First, a simple Weibull deterioration model considering the impacts of single attributes of bridge deck deterioration is developed, which is easily implementable. A Weibull distribution is found that calculates the probability that a bridge will decrease in condition rating given the amount of days it has been at that rating. The probability density function (PDF) of the log-normal distribution, $f(t)$, is shown as Equation 1.

$$f(t,\lambda,k) = \begin{cases} \frac{k}{\lambda}\left(\frac{t}{\lambda}\right)^{k-1} e^{-\left(\frac{t}{\lambda}\right)^{k}} & t \geq 0 \\ 0 & t < 0 \end{cases} \tag{1}$$

where t is the independent variable, in this case, CTT, and λ and k are the parameters of the Weibull distribution.

The probability of a CR to decrease for a bridge can be modeled by the cumulative distribution function. The equation for the cumulative density function of the Weibull distribution, $F(t)$, is shown as Equation 2.

$$(t) = 1 - e^{-\left(\frac{t}{\lambda}\right)^{k}} \tag{2}$$

The maximum likelihood estimation approach is used to estimate the parameters of the log-normal distribution.

It is possible to use the models developed above to determine the probability that a bridge deck will deteriorate given a single attribute. These individual models can further be combined using weighting factors to determine the probability that a bridge deck will deteriorate considering combinations of attributes. Since the contribution of these attributes to deterioration may not equal in practice, a weight factor can be applied to specific attributes such that that attribute can contribute more or less to the

deterioriation probability. This allows for expert input when determining the overall deterioration of a bridge. The function to calculate the combined deterioration probability is shown as in Equation 3.

$$C(t) = \sum_{i}^{N} \omega_i F_{i(t)} \tag{3}$$

where ω_i is the weight factor of ith attributes and N is the number of attributes considered.

The weights must be determined carefully based on experience. Expert knowledge is needed to reasonably allocate the weight of each attribute to make the final weighted deterioration probability close to reality. Once the weights are determined, the deterioration probability at a given condition rating after a specific sojourn time can be calculated using the log-normal distribution model. Then these deterioration probabilities will be weighted together to obtain the probability that a bridge will deteriorate.

ACCELERATED-FAILURE TIME MODEL

A more complicated model that utilizes all the data is used next. Survival data analysis aims at modeling the duration of time until an event, or failure, happens, defined as the sojourn time. The specific dependent variable being modeled in survival analysis is known as the hazard, which is defined as the probability of failure at a given time conditional on the fact that failure has not happened until that time. The hazard rate function $\lambda(t)$ can be defined as in Equation 4.

$$\lambda(t) = \frac{f(t)}{R(t)} \tag{4}$$

where $f(t)$ is the probability density function of the sojourn time defined as the probability that an event lasts at least until time t, and $R(t)$ is the reliability (or the survival) function of the sojourn time. Four approaches to modeling hazard with covariates exist: (1) parametric families, (2) accelerated failure time, (3) proportional hazards, and (4) proportional odds.

Parametric families estimate the parameters of an assumed distribution based on the covariates; however, they can be complex and difficult to interpret. Proportional hazards and proportional odds models assume that the hazard rate is scaled by a constant covariate. These proportional hazards assumptions can be restricting, since they imply that the covariates do not vary with time. On the other hand, accelerated failure time models assume that the covariates accelerate or decelerate the failure time. Hence, accelerated failure time models were chosen for this work due to their flexibility.

The general form of an accelerated failure time model assumes that the logarithm of the failure time can be expressed as a linear function of covariates as follows:

$$\log(t) = \overline{\boldsymbol{X}}\overline{\boldsymbol{\beta}} + \beta_0 \tag{5}$$

where: $\overline{\boldsymbol{X}} = [1, X_2, .., X_k\,]$ is the vector of covariates, $\overline{\boldsymbol{\beta}} = [\beta_1, \beta_2, .., \beta_k\,]$ is the vector of regression coefficients, and β_0 is the random error term with a given probability distribution function. The distribution of the random error determines the resulting shape of the hazard and reliability function. In this study, the error term is assumed to follow the generalized gamma distribution (GGD). Below, the steps to modify the accelerated failure time methodology to represent a GGD are described.

The probability density function of a standard GGD is shown in Equation 6.

$$f(t) = \frac{\beta}{\Gamma(k)\theta}\left(\frac{t}{\theta}\right)^{k\theta-1} e^{-\left(\frac{t}{\theta}\right)^{\beta}} \tag{6}$$

where, $\Gamma(k)$ is the gamma function as shown below:

$$\Gamma(k) = \int_0^{\infty} s^{k-1}e^{-s}\, ds \tag{7}$$

The standard GGD is simple; however, the parameters cannot be easily estimated. Hence, this is reparametrized according to Lawless (2011) using new parameters μ, σ, λ as below:

$$\mu = ln(\theta) + \frac{1}{\beta} ln\left(\frac{1}{\lambda^2}\right) \tag{8}$$

$$\sigma = \frac{1}{\beta\sqrt{k}} \tag{9}$$

$$\lambda = \frac{1}{\sqrt{k}} \tag{10}$$

Hence, the updated PDF distribution with the new parameters is shown in Equation 11:

$$f(t) = \begin{cases} \frac{|\lambda|}{\sigma t}\frac{1}{\Gamma\left(\frac{1}{\lambda^2}\right)} e^{\left[\frac{\lambda\frac{ln(t)-\mu}{\sigma}+ln\left(\frac{1}{\lambda^2}\right)-e^{\lambda\frac{ln(t)-\mu}{\sigma}}}{\lambda^2}\right]} & \lambda \neq 0 \\ \frac{1}{t\sigma\sqrt{2\pi}} e^{-\frac{1}{2}\left(\frac{ln(t)-\mu}{\sigma}\right)^2} & \lambda = 0 \end{cases} \tag{11}$$

Then, the reliability function can be determined as shown in Equation 12:

$$R(t) = 1 - \int_0^t f(x)dx = \begin{cases} 1 - \Gamma_I\left(\frac{1}{\lambda^2}; \frac{e^{\lambda\frac{ln(t)-\mu}{\sigma}}}{\lambda^2}\right) & \lambda > 0 \\ 1 - \Phi\left(\frac{ln(t)-\mu}{\sigma}\right) & \lambda = 0 \\ \Gamma_I\left(\frac{1}{\lambda^2}; \frac{e^{\lambda\frac{ln(t)-\mu}{\sigma}}}{\lambda^2}\right) & \lambda < 0 \end{cases} \tag{12}$$

Note that the GGD can be simplified to other well-known distributions such as the Weibull distribution ($\boldsymbol{\lambda}$=**1**), exponential distribution ($\boldsymbol{\lambda}$=**1** & $\boldsymbol{\sigma}$=**1**), lognormal distribution ($\boldsymbol{\lambda}$=**0**), or gamma distribution ($\boldsymbol{\lambda}$=$\boldsymbol{\sigma}$). To incorporate the attributes into the model, first the independent variable t is normalized to $Z(t)$:

$$Z(t) = \frac{ln(t)-\mu}{\sigma} = \frac{1}{\sigma} ln\left(\frac{t}{\mu}\right) \tag{13}$$

From this normalized expression, it can be found that μ is the scale parameter and λ and σ are shape parameters. So, the scale parameter, μ, can be replaced with a linear combination of covariates as shown in Equation 14.

$$\mu = e^{\overline{\boldsymbol{\beta}}\boldsymbol{x}} \tag{14}$$

Then, the GGD becomes an AFT-GGD, the PDF becomes:

$$f\left(t, \boldsymbol{x} | \mu, \lambda, \overline{\boldsymbol{\beta}}\right) = \begin{cases} \dfrac{|\lambda|}{e^{\overline{\boldsymbol{\beta}}\boldsymbol{x}} t} \dfrac{1}{\Gamma\left(\frac{1}{\lambda^2}\right)} e^{\left[\frac{\lambda \frac{ln(t) - e^{\overline{\boldsymbol{\beta}}\boldsymbol{x}}}{e^{\overline{\boldsymbol{\beta}}\boldsymbol{x}}} + ln\left(\frac{1}{\lambda^2}\right) - e^{\lambda \frac{ln(t) - e^{\overline{\boldsymbol{\beta}}\boldsymbol{x}}}{e^{\overline{\boldsymbol{\beta}}\boldsymbol{x}}}}}{\lambda^2}\right]} & \lambda \neq 0 \\ \dfrac{1}{t e^{\overline{\boldsymbol{\beta}}\boldsymbol{x}} \sqrt{2\pi}} e^{-\frac{1}{2}\left(\frac{ln(t) - e^{\overline{\boldsymbol{\beta}}\boldsymbol{x}}}{e^{\overline{\boldsymbol{\beta}}\boldsymbol{x}}}\right)^2} & \lambda = 0 \end{cases} \tag{15}$$

where, $\boldsymbol{x}$ is a vector of attribute values, $\overline{\boldsymbol{\beta}}$ is a vector of coefficients for different attributes, t is the independent variable, and σ, λ are shape parameters.

Estimating the Parameters

The parameters of the model, σ, λ *and* $\overline{\boldsymbol{\beta}}$, are estimated using an MCMC with Bayesian inference. To do so, first the likelihood function, which describes the probability of obtaining the observations in a dataset given the parameter estimates, needs to be estimated. The likelihood function is composed of two parts depending on the available sojourn time data: (1) the likelihood function of the uncensored data (i.e., data where the observation period covers both the beginning and the end of a condition rating) and (2) the likelihood function of censored data (i.e., either the beginning or the end of a condition is not observed). The likelihood function of the uncensored data can be calculated as the probability density function, while the likelihood function of the censored data can be calculated using the reliability function. Thus, the final likelihood function of the whole dataset can be expressed as a product of the probability density functions of the uncensored data and the reliability functions of the censored data, see Equation 16.

$$P\left(D \middle| \sigma, \lambda, \overline{\boldsymbol{\beta}}\right) = \prod_{i \in D_u} f\left(t_i | \sigma, \lambda, \overline{\boldsymbol{\beta}}\right) \prod_{i \in D_C} R\left(t_i | \sigma, \lambda, \overline{\boldsymbol{\beta}}\right) \tag{16}$$

where, $D_u$is the data set of all uncensored data, D_C is the data set of all censored data, f is the probability density function, and R is the reliability function.

The MCMC method assumes that the GGD parameters σ, λ and the coefficients for the covariates, $\overline{\boldsymbol{\beta}}$, initially follow an unknown distribution. Hence, to be able to estimate these coefficients, a prior distribution for these parameters is estimated. In this study, the prior distributions are assumed to be uniform, as shown in Equation 17.

$$\sigma \sim Beta(a_\sigma, b_\sigma), \lambda \sim Beta(a_\lambda, b_\lambda), \beta_i \sim Beta\left(a_{\beta_i}, b_{\beta_i}\right) \tag{17}$$

where, β_i are elements of $\overline{\boldsymbol{\beta}}$, a_*, b_* are hyper-parameters of the prior distribution, there are assumed to follow a uniform distribution to initialize the updating approach.

The MCMC method calculates a posterior distribution using Bayesian inference as below:

$$f_X(\sigma, \lambda, \overline{\boldsymbol{\beta}}|D) = kP(\overline{D}|\sigma, \lambda, \overline{\boldsymbol{\beta}})f_X(\sigma, \lambda, \overline{\boldsymbol{\beta}}) \tag{18}$$

where $f_X(\sigma, \lambda, \overline{\boldsymbol{\beta}})$is the PDF of the prior distribution of parameters, $P(\overline{D}|\sigma, \lambda, \overline{\boldsymbol{\beta}})$is the likelihood function that data D is observed, $f_X(\sigma, \lambda, \overline{\boldsymbol{\beta}}|D)$ is the PDF of the parameters after observing data D, and k is a normalizing constant.

Since there is no analytical expression of the posterior distribution function, the distribution of the parameters σ, λ $\overline{\boldsymbol{\beta}}$ can be calculated using a heuristic algorithm or MCMC sampling. Here a standard Metropolis Hasting MCMC method is used. The MCMC method will generate samples and decide whether to accept it for the final distribution calculations with a probability equal to the acceptance ratio. The standard Metropolis Hasting MCMC method has an acceptance ratio that is determined using Equation 19.

$$\alpha = min\left(1, \frac{f(x')p(x|x')}{f(x)p(x'|x)}\right) \tag{19}$$

where, the x' is the new sample and x is the current sample, $f(x')$ and $f(x)$ is the PDF of new sample, x', and current sample, x, respectively; $p(x|x')$ is the transition probability from sample x' to x, and similar as $p(x'|x)$. This acceptance ratio is chosen to ensure that samples with higher PDF values are more likely to be accepted, thus allowing the samples to cluster around the optimal value.

When the sample dimension is high, the new sample, x', can easily drift away from the optimal solution, which will lead to a very small $f(x')$ and thus have a low acceptance ratio. In order to increase the acceptance ratio and improve the efficiency of the method, the standard acceptance ratio was slightly modified to accelerate the sampling process, see Equation 20.

$$\alpha = min\left(1, \frac{log(1 + f(x'))p(x|x')}{log(1 + f(x))p(x'|x)}\right) \tag{20}$$

Bayesian Updating

The above method can be implemented whether or not historical information is available. When there is no historical information, a uniform distribution can be assumed as the prior distribution for each parameter. The posterior distribution of parameters is calculated based on the new data and the assumed prior distribution as in Equation 21.

$$\begin{aligned} f_X(\sigma, \lambda, \boldsymbol{\beta}|D) \propto Beta(a_\sigma, b_\sigma) \times Beta(a_\lambda, b_\lambda) \times \prod_i Beta(a_{\beta_i}, b_{\beta_i}) \\ \times \prod_{i \in D_u} f(t_i|\sigma, \lambda, \boldsymbol{\beta}) \prod_{i \in D_C} R(t_i|\sigma, \lambda, \boldsymbol{\beta}) \end{aligned} \tag{21}$$

where, the $\prod_{i \in D_u} f(t_i|\sigma, \lambda, \boldsymbol{\beta}) \prod_{i \in D_C} R(t_i|\sigma, \lambda, \boldsymbol{\beta})$ is the likelihood function of new data, $Beta(a_\sigma, b_\sigma) \times Beta(a_\lambda, b_\lambda) \times \prod_i Beta(a_{\beta_i}, b_{\beta_i})$ is an assumed prior distribution of each parameters.

When a model already exists, the updated parameters are calculated using MCMC as described above utilizing only the newly available data. However, the posterior distribution calculated using the previously available data becomes the prior distribution for the new model, see Equation 22.

$$f_X(\sigma,\lambda,\boldsymbol{\beta}|D) \propto f(\sigma,\lambda,\boldsymbol{\beta}) \times \prod_{i\in D_u} f(t_i|\sigma,\lambda,\boldsymbol{\beta}) \prod_{i\in D_C} R(t_i|\sigma,\lambda,\boldsymbol{\beta}) \tag{22}$$

where, $f(\sigma,\lambda,\boldsymbol{\beta})$ is the distribution of parameters calculated based on previously available data, and now is treated as the prior distribution in the updating process, and $f_X(\sigma,\lambda,\boldsymbol{\beta}|D)$ is the distribution of the parameters that combine the previously available data as well as the newly available data.

Addressing Computational Issues

There are some computational limitations to estimating the above described model specifically for large datasets. Three major concerns are: (1) the likelihood function approaches 0 as the likelihood for more data is considered, (2) the likelihood function is fairly flat around the optimal solution, and (3) the AFT-GGD approaches infinity when the λ is small. The modifications to the model to address these issues are discussed below.

Likelihood function

As the number of available data increases, the likelihood value goes to 0 and the log-likelihood value to infinity. This leads to the MCMC method failing to converge. See for example Figure 2, which shows the likelihood distribution as a function of μ and λ while keeping σ constant for an illustration of this problem.

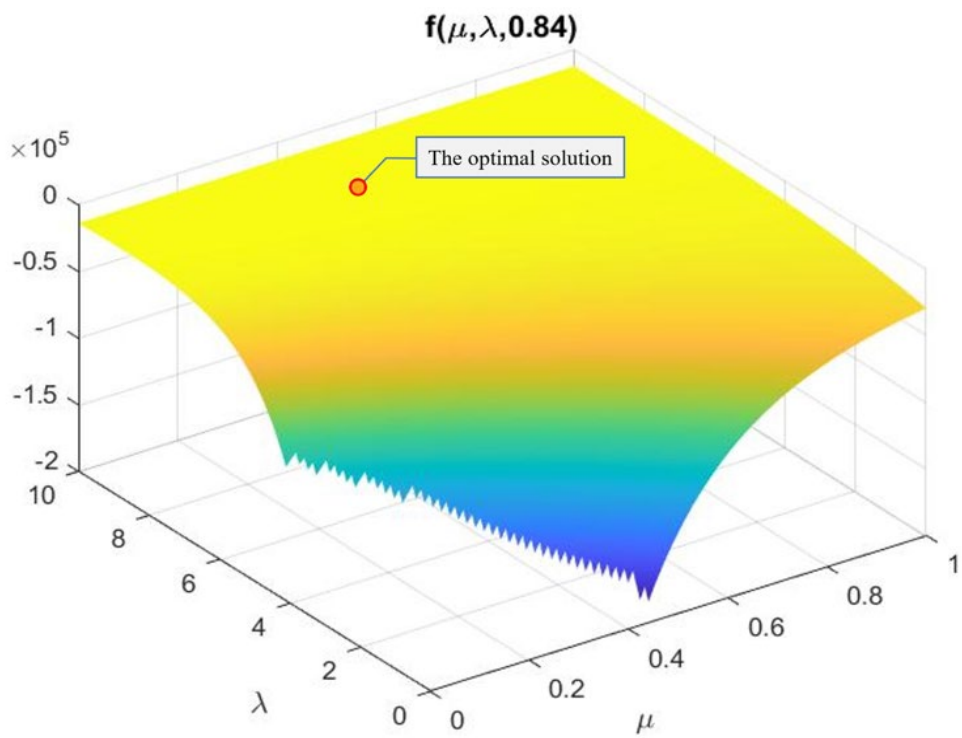

Figure 2. Likelihood distribution of the generalized gamma distribution.

From Figure 2, it can be observed that: (1) when $\lambda\ or\ \mu$ decreases, the likelihood function approaches infinity, and (2) the likelihood function is flat around the optimal solution (shown by the red circle as estimated by maximum likelihood estimation). Both of these issues hinder the ability of the MCMC method to converge. Hence, the likelihood function is transformed into a logarithmic space as shown in Equation 23.

$$Log\_Likelihood = \sum_{d_u \in D_{uncesored}} log\big(f(d_u)\big) + \sum_{d_c \in D_{censored}} \log\big(f(d_c)\big) \tag{23}$$

Next, the maximum log-likelihood value for all parameters was calculated and subtracted from the log-likelihood value. Finally, the following likelihood function was used in the MCMC calculations:

$$L = exp\left(Log\_Likelihood - \max_{\forall\, \mu,\, \sigma, \lambda}(Log\_Likelihood)\right) \tag{24}$$

Addressing issues with the gamma function

In the PDF function of the GGD shown in Equation 15, when λ approaches 0, $\frac{1}{\lambda^2}$ starts approaching infinity, and the gamma function may overflow. Tests had shown that when λ is less than 0.05, the gamma function will return infinity in any common language (e.g., Python, MATLAB).
In order to overcome this overflow problem, the function shown in Equation 15 was transformed. Firstly, the gamma function can be calculated as below.

$$\Gamma\left(\frac{1}{\lambda^2}\right) = e^{log\left(\Gamma\left(\frac{1}{\lambda^2}\right)\right)} = e^{\sum_{i=1}^{k} log\left(\frac{1}{\lambda^2}-i\right)+log\left(\Gamma\left(\frac{1}{\lambda^2}-\mathrm{k}\right)\right)} \tag{25}$$

Using Equation 25 and substituting it in Equation 15, the PDF can be transformed as Equation 26 (when $\lambda \neq 0$):

$$f = \frac{|\lambda|}{e^{\beta x} t} e^{\left[\frac{\lambda \frac{ln(t)-e^{\beta x}}{e^{\beta x}} + ln\left(\frac{1}{\lambda^2}\right) - e^{\lambda \frac{ln(t)-e^{\beta x}}{e^{\beta x}}}}{\lambda^2} - \sum_{i=1}^{k} log\left(\frac{1}{\lambda^2}-i\right)+log\left(\Gamma\left(\frac{1}{\lambda^2}-k\right)\right)\right]} \tag{26}$$

After this transformation, the optimal solution has a high likelihood and the distribution of the new likelihood is shown in Figure 3. It can be seen that with this transformation non-optimal solutions have a likelihood value close to zero, whereas the optimal solution has a likelihood value that is distinctly different, improving the computational efficiency of the MCMC method.

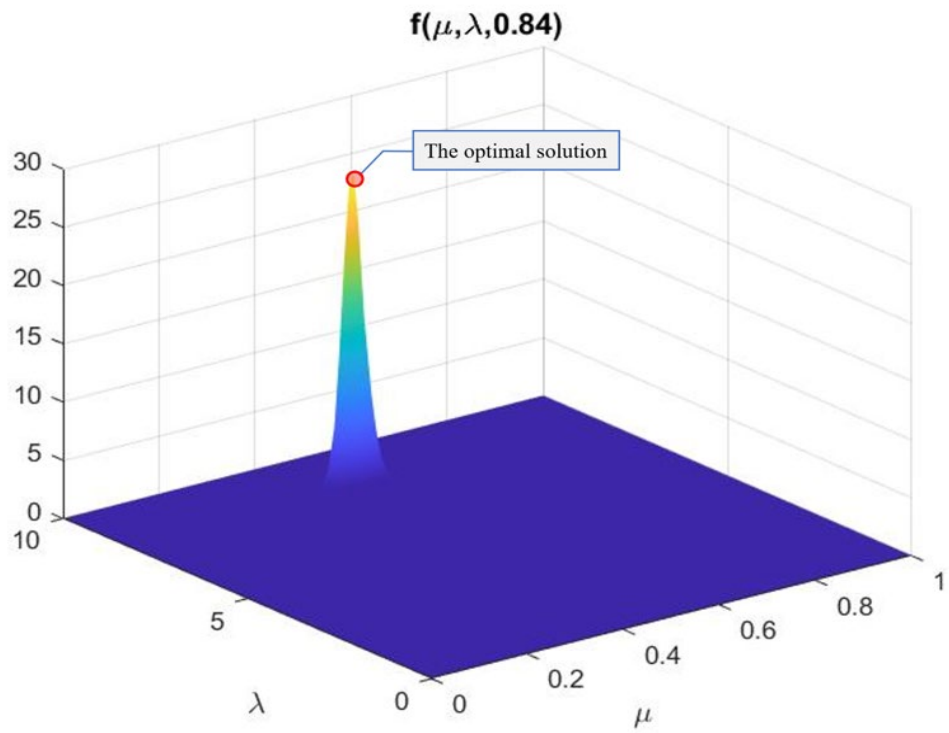

Figure 3. Transformed likelihood distribution of the generalized gamma function.

CHAPTER 4

Data Processing and Exploration

INTRODUCTION

Approximately 51,463 bridge deck inspection CRs stemming from over 22,000 bridges in Pennsylvania were utilized in order to model the data (PennDOT, 2009). The time that a bridge deck spends in a given condition rating, the sojourn time, was extracted from the data. In other words, the time difference between two changes in the condition rating for a given bridge deck was calculated. Due to the large volume of data, filters were applied to ensure accuracy and consistency to compare deck ratings and sojourn times. Filters were also used to lower the standard deviation of the data. These filters include:

(a) removing miscoded, duplicate, and mismatching data;
(b) removing data if a bridge deck did not maintain a particular condition rating for two consecutive inspection points;
(c) removing data with more than 1,500 days between inspections;
(d) removing data for bridges without at least three total inspection points; and
(e) removing data if bridge deck condition reduced by more than two ratings in between inspections.

The available attributes from BMS2 are summarized in Table 1.

The inspection data were first preprocessed and cleaned. First, if a CR increased or decreased for only a single inspection, this data point was corrected to the before and after condition rating. Also, data that did not have an inspection data were discarded. If the CR was not recorded for two consecutive inspections, data were discarded (to eliminate possible errors in CR reporting). Moreover, if there were more than 1,500 days (4 years) between inspections and the CR changes, this data point was discarded (since the actual deterioration time would be unknown). Finally, if the CR changed more than two levels (higher or lower) in between inspections it was assumed that either a maintenance activity or a traffic accident had happened. These data were treated as censored, and an indicator variable "Event" was included for these data.

After cleaning the raw data, valid information for 18,354 bridges was obtained, and a total of 44,086 sojourn times were extracted and classified given the CR. In order to choose a suitable model to predict the lifecycle performance of bridge decks, a non-parametric analysis of these sojourn times was first conducted. First, summary statistics for the distribution of the sojourn times were determined as shown in Table 2.

Table 1. Attributes description and values distribution.

Attributes	Summary	Values (Counts)*
DISTRICT	District number	District 1 (2707); District 2 (2102); District 3 (3171); District 4 (2200); District 5 (2215); District 6 (2912); District 8 (5369); District 9 (3497); District 10 (2443); District 11 (2672); District 12 (2817).
DEPT_DKSTRUC_TYP	Deck structure type	Concrete - Reinforced (26324);
DEPT_MAIN_MATERIAL_TYPE	Main materials type	Steel (8531); Concrete (Cast in Place) (6205); Concrete (Precast) (537); Prestressed Precast Concrete (P/S) (15774); Concrete Encased Steel (982).
DEPT_MAIN_PHYSICAL_TYPE	Physical makeup of the main span of the structure	Reinforced (6744); Pretensioned (15600); Rolled Sections (4787); Rolled Sections with Cover Plates (1174); Combination, Rolled Sections/Cover-Plates (334); Other (3313).
DEPT_MAIN_SPAN_INTERACTION	Span interaction for the main span of the structure	Simple, Non-Composite (12042); Simple, Composite (15377); Continuous, Non-Composite (882); Continuous, Composite (2751); Other (1053).
DEPT_MAIN_STRUC_CONFIG	Structural configuration for the main span of the structure	Slab (Solid) (2378); T-Beams (3985); I Beams (11653); Box Beam - Single (5681); Box Beam - Adj (6614); I-Welded Beams (410); Girder Weld/Deck (722).
DK_PROTECT	Deck protection type	None (18171); Epoxy Coated Reinforcing (12439); Galvanized Reinforcing (461); Unknown (804).
DECK_REBAR_TYPE	Deck rebar type	Bare Rebar Type (12960); Galvanized Rebar Type (561); Epoxy Rebar Type (11738); Unknown (6794).
MAIN_SPANS	Main bridge spans (number of spans in main unit)	1 (20209); 2 (4954); 3 (4167); 4 (1416); 5 (585).
DKMEMBTYPE	Waterproofing membrane on the bridge main span	None (26722); Preformed Fabric (3816); Other (368).
DKSURF_TYPE	Wearing surface types on the bridge main span	Concrete (14137); Concrete Overlay (3406); Epoxy Overlay (974); Bituminous (13340).
HAPPENED	If special event happened	Sharply Decrease (3497); Normal (22332); Sharply Increase (6212).
LENGTH	Bridge length	Total overall length of the bridge
DECK WIDTH	Bridge deck width.	Bridge deck width
ADTT	Average daily truck traffic	Average daily truck traffic

*The Values (Counts) only show the values whose count is larger than 1% of the whole dataset.

Table 2. Statistic of sojourn times (in days) of bridge decks.

Condition Rating	Censored Count	Censored Mean	Censored Std	Complete Count	Complete Mean	Complete Std
CR 1	19	2,809	2,509	2	1,040	348
CR 2	104	1,690	1,263	13	1,818	1,124
CR 3	1,007	2,022	1,709	170	2,034	1,421
CR 4	3,132	3,197	2,410	783	2,581	1,717
CR 5	6,016	4,010	2,759	2,317	2,935	1,794
CR 6	7,264	4,024	2,622	3,865	2,977	1,719
CR 7	8,636	3,957	2,603	3,817	3,054	1,760
CR 8	3,234	2,610	1,927	2,612	2,501	1,443
CR 9	654	1,420	1,106	381	1,747	1,049
Total	30,066			13,960		

Looking at Table 2, it can be observed that only a small number of bridges deteriorated to CR 4 or worse, as typically when a deck enters CR 4, it is designated for an immediate replacement and CR 4 signifies the end of the useful service life. To better understand the distribution of both complete and right-censored sojourn times a violin plot, as shown in Figure 4, was utilized.

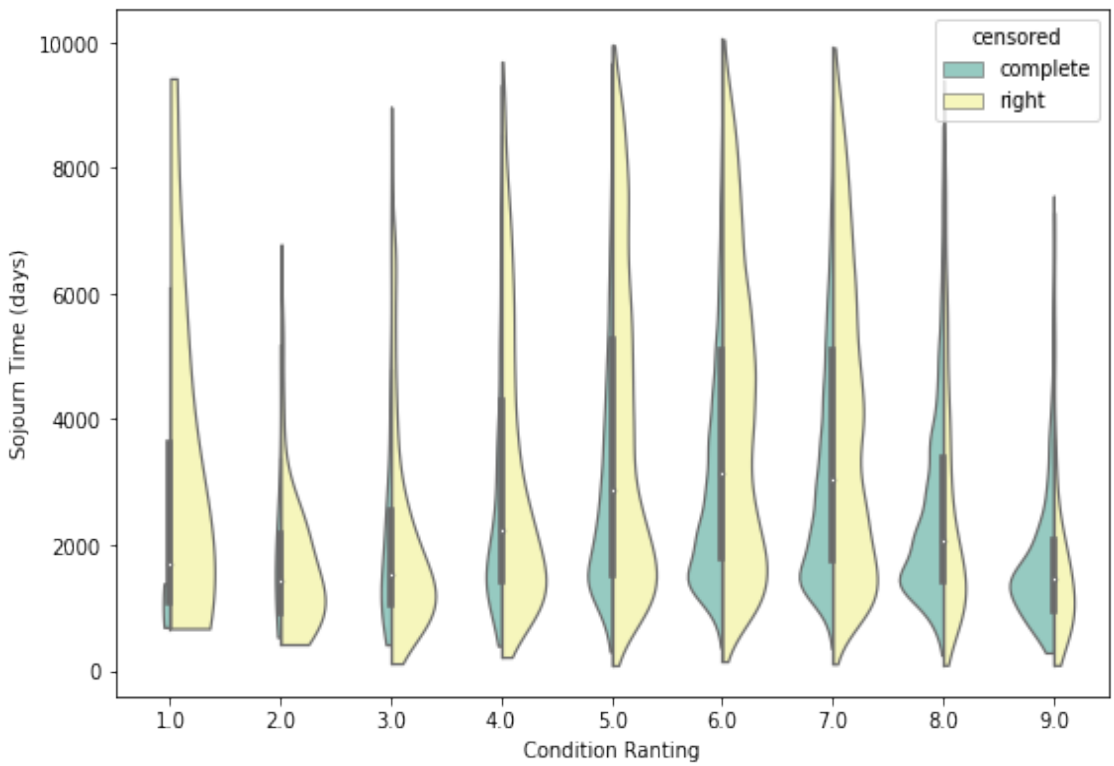

Figure 4. Distribution of complete and right-censored data for different CRs.

From Figure 4, it can be seen that complete data were mostly available for CR 5 to CR 8, and the distribution of complete data follows a bathtub shape. Due to the lack of data for CRs 3, 2, and 1, this study only utilized data for bridge decks with CR greater than 3.

First, only the non-censored data were explored. The mean sojourn time for a bridge was found to be 2,849 days (7.7 years), with a skewed right distribution and a skewness (σ) value of 0.7. The average standard deviation for the data is 1,621 days (4.4 years). The typical lifecycle of a bridge deck is as follows: a short sojourn time at CR 9, gradually increasing sojourn times at CR 8, and the largest sojourn times at CR 7 and CR 6, and then gradually decreasing sojourn times until the bridge is no longer serviceable. While this trend is generally observable, the duration each bridge deck spends in each CR depends on many of the physical attributes of the bridge (e.g., the amount of truck traffic the bridge is exposed to and its year of construction). While sojourn time can be a good reflection of the reliability of a bridge deck, it is significantly impacted by the amount of truck traffic that a bridge deck experiences. The average daily truck traffic varies a lot across different bridges. Moreover, the expected average daily truck traffic will influence the design of a bridge deck. Consider the deck surface type as an example. Looking at the data, while 55.1% of bridges with ADTT less than 1,000 vehicles per day used a bituminous surface type, only 23.8% of bridges with ADTT larger than 1,000 veh/day used bituminous and instead 65.5% of them used a concrete surface. This indicates that the average daily truck traffic should be taken into consideration when analyzing the reliability of a bridge. Hence, in addition to the sojourn times, the cumulative truck traffic (CTT), defined as the product of the sojourn time and average daily truck traffic, is also analyzed. In other words, the cumulative truck traffic experienced until a change in the CR is analyzed as a function of the different attributes of the bridge deck.

REBAR TYPE

Three different rebar types used in bridge decks were compared: bare, epoxy-coated, and galvanized. The average sojourn for all three rebar types is approximately 7 years. However, the bare rebar type slightly outperformed the other two types for most CRs except for CR 8, see Figure 5a. On the other hand, there is a significant difference between the three rebar types in terms of number of bridges and average daily truck traffic, see Figures 5b and c, respectively. From Figure 5b, it can be observed that there are few bridge decks that use galvanized rebar across PA, and most of the bridge decks with bare rebar are in CR 6 or below. On the other hand, many of the bridges with larger CRs (e.g., CR 7 and above) have epoxy rebar. Furthermore, Figure 5c shows that the average daily truck traffic on bridge decks with galvanized rebar or epoxy rebar is much higher than on bridge decks with bare rebar at CR 6 and CR 7. This indicates that in areas with large truck traffic, bridge decks were more often designed with epoxy or galvanized rebars. Note that the data for CR 9 are not reliable since too few bridges are inspected in the condition rating, especially for bridge decks with bare rebar. Thus, considering the cumulative truck traffic until a change in CR, Figure 5d shows that bridge decks with epoxy or galvanized rebar have a higher reliability compared to the bare rebar bridges. However, the reliability of bridge decks with epoxy or galvanized rebar decreases faster than bridge decks with bare rebar when the bridge deck starts to deteriorate to CR 5 or lower. The reason is that galvanized coated rebar does not perform as well when concrete is cracked, and at this condition rating most bridge decks have cracks and delamination (Prozzi and Madanat, 2000; Guler and Madanat, 2011).

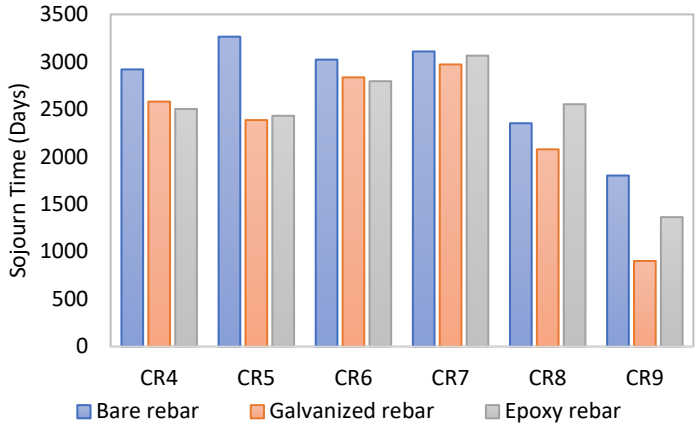

(a) Sojourn Time

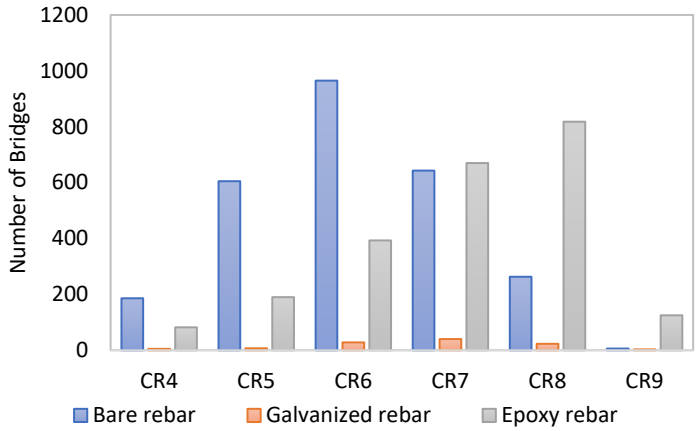

(b) Number of Bridges

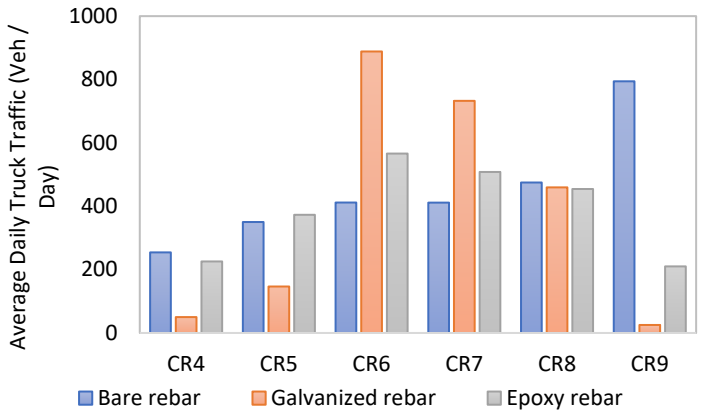

(c) Average Daily Truck Traffic

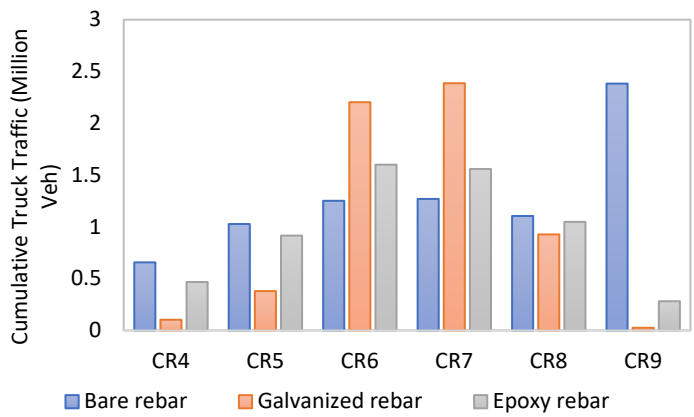

(d) Cumulative Truck Traffic

Figure 5. Distribution for rebar type by condition rating of: (a) sojourn time, (b) number of bridges, (c) average daily truck traffic, and (d) cumulative truck traffic.

SPAN NUMBER

Single-span bridges were compared to multi-span bridges in order to see trends in deterioration. The average deck length of a single-span bridge is 42 ft, compared to 278 ft for a multi-span bridge. The sojourn time distributions for the two types of bridges for different CR values are shown in Figure 6a. From the sojourn time distribution, it can be found that for most condition ratings a single-spanned bridge has a longer sojourn time than its multi-spanned counterpart, with the greatest difference being a 21% increase in sojourn time at a condition rating of 9. However, this does not necessarily indicate that a single-span bridge is more reliable than a multi-span bridge. Considering the number of bridges (see Figure 6b) and the average daily truck traffic (see Figure 6c), it can be seen that while there are more single-span bridges, the multi-span bridges carry many more trucks. This implies that the multi-span bridges are mostly constructed in areas with heavy truck traffic. Finally, Figure 6c shows that at all CRs, multi-span bridges can support a larger cumulative truck traffic compared to single-span bridges before deteriorating.

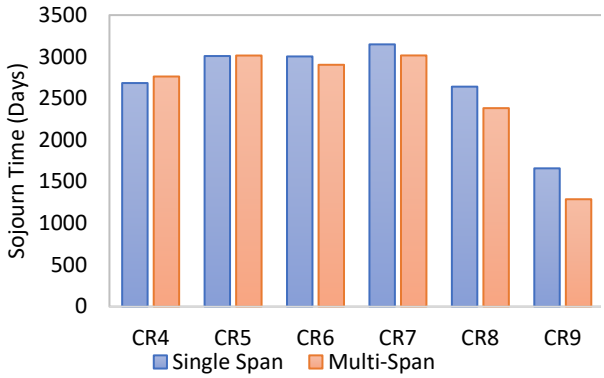

(a) Sojourn Time

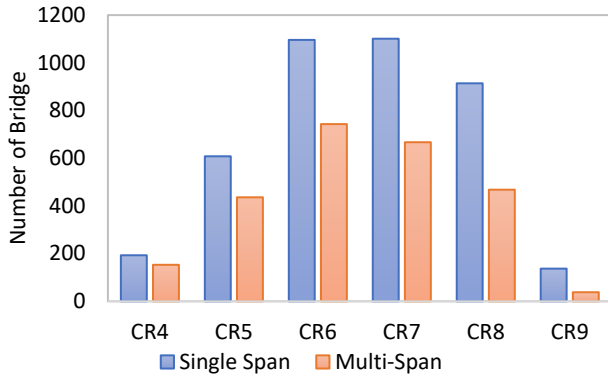

(b) Number of Bridges

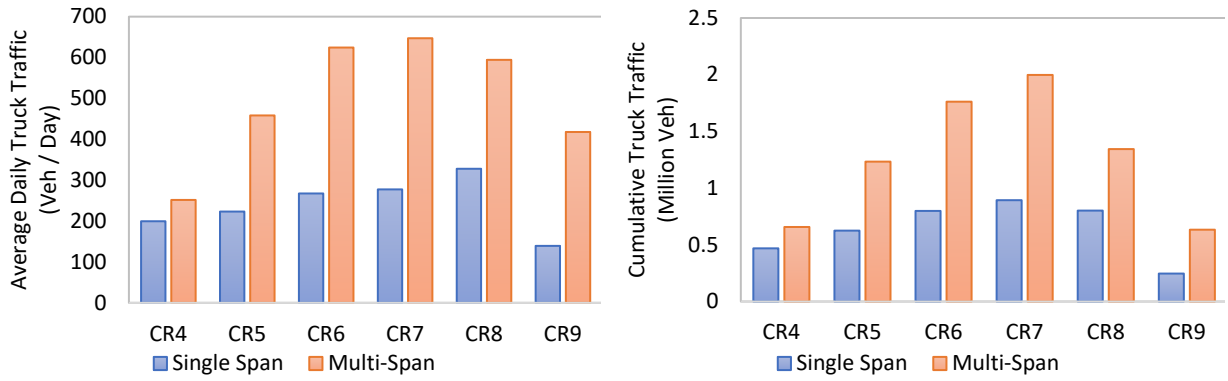

(c) Average Daily Truck Traffic (d) Cumulative Truck Traffic

Figure 6. Distribution for span type by condition rating of: (a) sojourn time, (b) number of bridges, (c) average daily truck traffic, and (d) cumulative truck traffic.

SURFACE TYPE

Overlays are used to remedy spalling and cracking for deteriorated bridge surfaces. They are used to repair the deck surface without having to make significant repairs to the bridge, and an overlay will typically increase a bridge's condition rating and also extend its service life. Comparing the sojourn times for the three different overlay materials used (concrete, asphalt, and epoxy) it can be seen that bridge decks that have an asphalt overlay have on average an 8.8% greater sojourn time, see Figure 7a. Moreover, this difference increases to 30.3% when inspecting bridges at ratings of 8 or 9. However, only a small number of bridges have an epoxy overlay (see Figure 7b) and these bridges have a larger daily truck traffic compared to bridges with concrete or asphalt overlay (see Figure 7c). Hence, when considering the cumulative truck traffic it can be seen that bridges with epoxy overlay have the highest reliability, while bridges with asphalt overlay have the lowest reliability (see Figure 7d). While bituminous acts as a protective layer that prevents accelerated deterioration (Tabatabai et al., 2011), once the bridge has been exposed to external elements such as salts and weathering, asphalt experiences similar failure methods, including fatigue cracking, rutting, and stripping. Hence, the asphalt overlay does not perform as well as epoxy overlay.

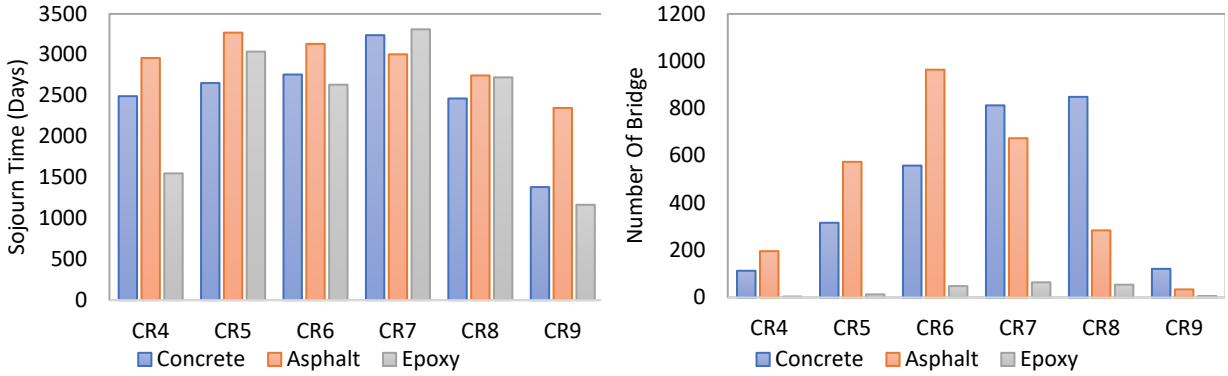

(a) Sojourn Time (b) Number of Bridges

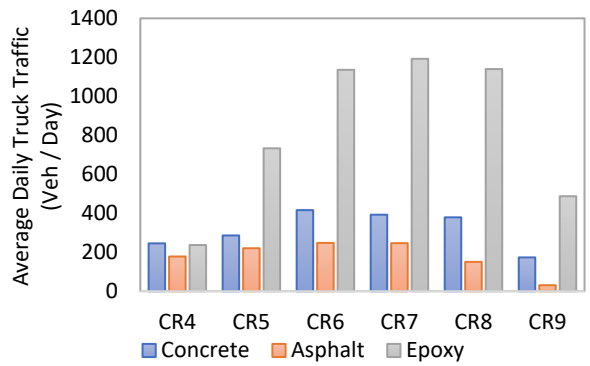

(c) Average Daily Truck Traffic

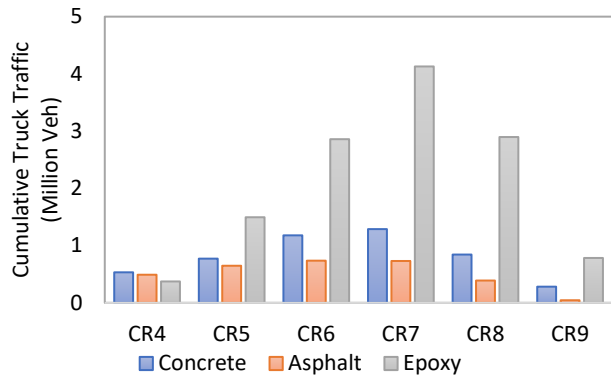

(d) Cumulative Truck Traffic

Figure 7. Distribution for surface type by condition rating of: (a) sojourn time, (b) number of bridges, (c) average daily truck traffic, and (d) cumulative truck traffic.

YEAR CONSTRUCTED

The data provided by PennDOT has inspections that started in 1985. These bridges can be grouped into three periods based on their construction year: (1) before 1943, (2) 1943-1980, and (3) post-1980 (see Figure 8).

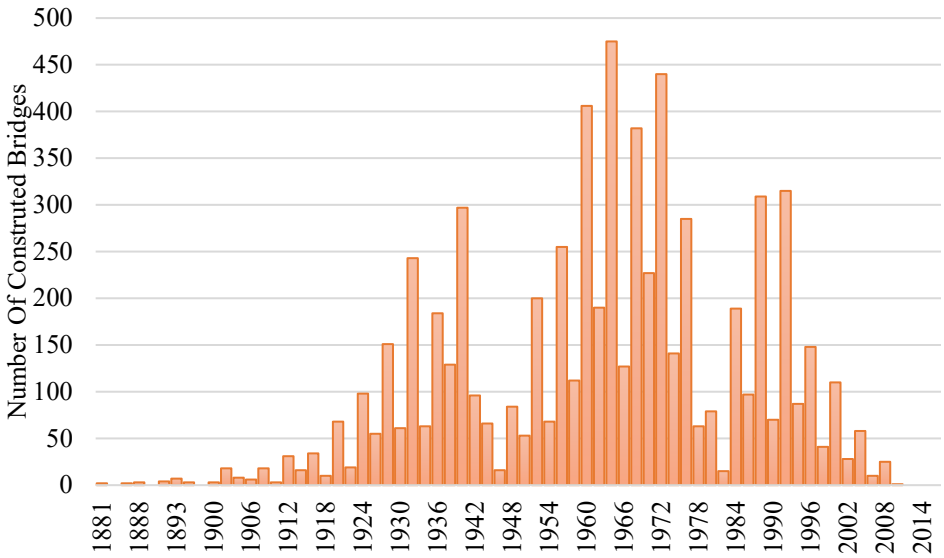

Figure 8. Construction year of all bridges.

As technology developed and the traffic environment changed, the bridges constructed during these different periods have different performances. Based on the results, as expected the older bridges spent more time in lower condition ratings and the newer bridges spent more time in higher condition ratings (see Figure 9a). Additionally, there were more data from lower condition ratings from older bridges and more data from newer bridges in high condition ratings (see Figure 9b). However, the data show that the bridges built between 1943 and 1980 are the ones that carry most of the truck traffic (see Figure 9c). Hence, when

comparing the cumulative traffic load in each condition rating it can be seen that the most reliable bridges are those that were built between 1943 and 1980 (see Figure 9d). This is likely due to the generally larger truck traffic carried by these bridges.

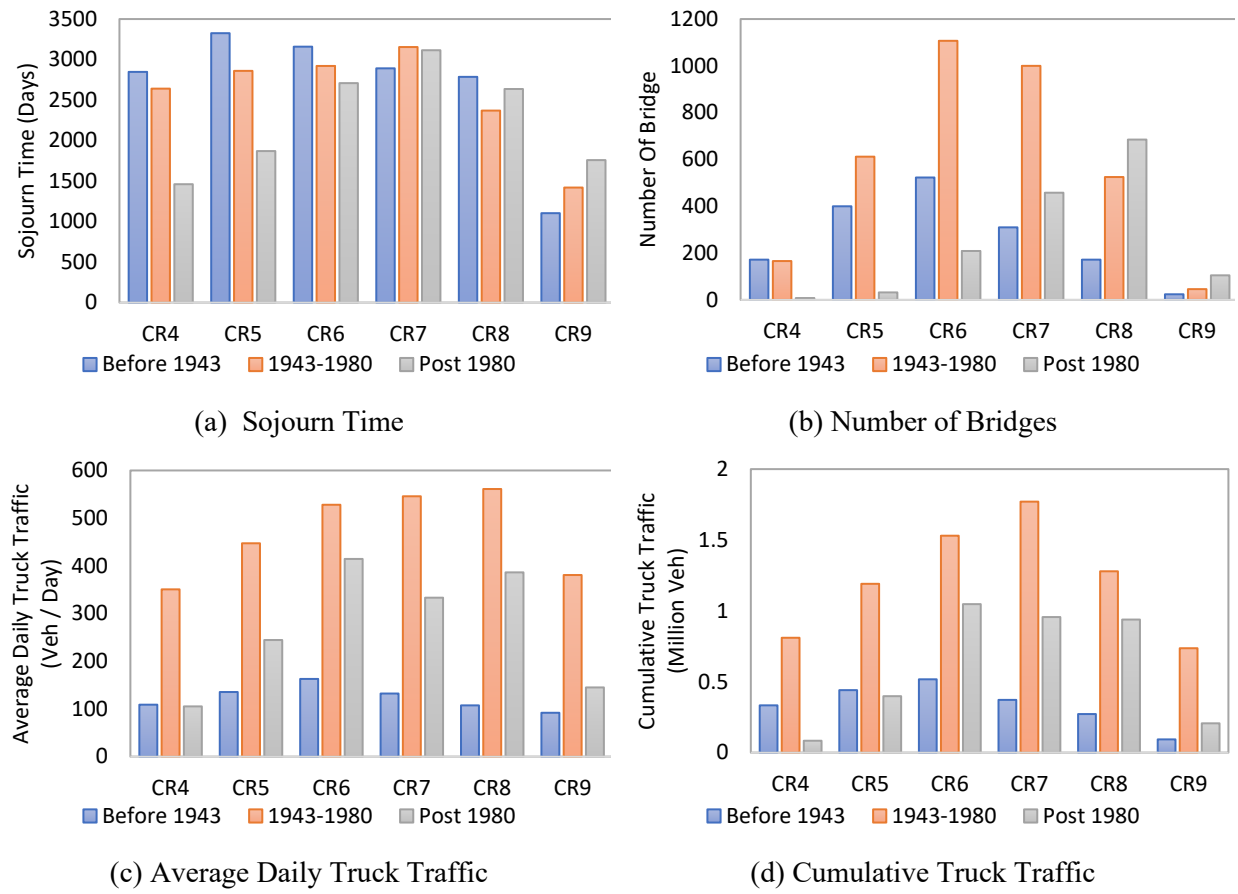

Figure 9. Distributions for different construction years by condition rating of: (a) sojourn time, (b) number of bridges, (c) average daily truck traffic, and (d) cumulative truck traffic.

Based on the Kaplan-Meier estimator (Kaplan and Meier, 1958), the reliability of different CRs was calculated by incorporating all uncensored data. The non-parametric reliability for duration, t, was calculated as shown in Equation 27.

$$\hat{R}(t) = \prod_i \frac{n_i - m_i}{n_i} \tag{27}$$

where, n_i is the number of sojourn times that are greater than or equal to time t_i and m_i is the number of sojourn times that are exactly equal to t_i.

The real deterioration pattern calculated using the Kaplan-Meier estimator are plotted in Figure 10 as a blue curve. The fitting curve of each distribution is plotted as an orange curve in Figure 10.

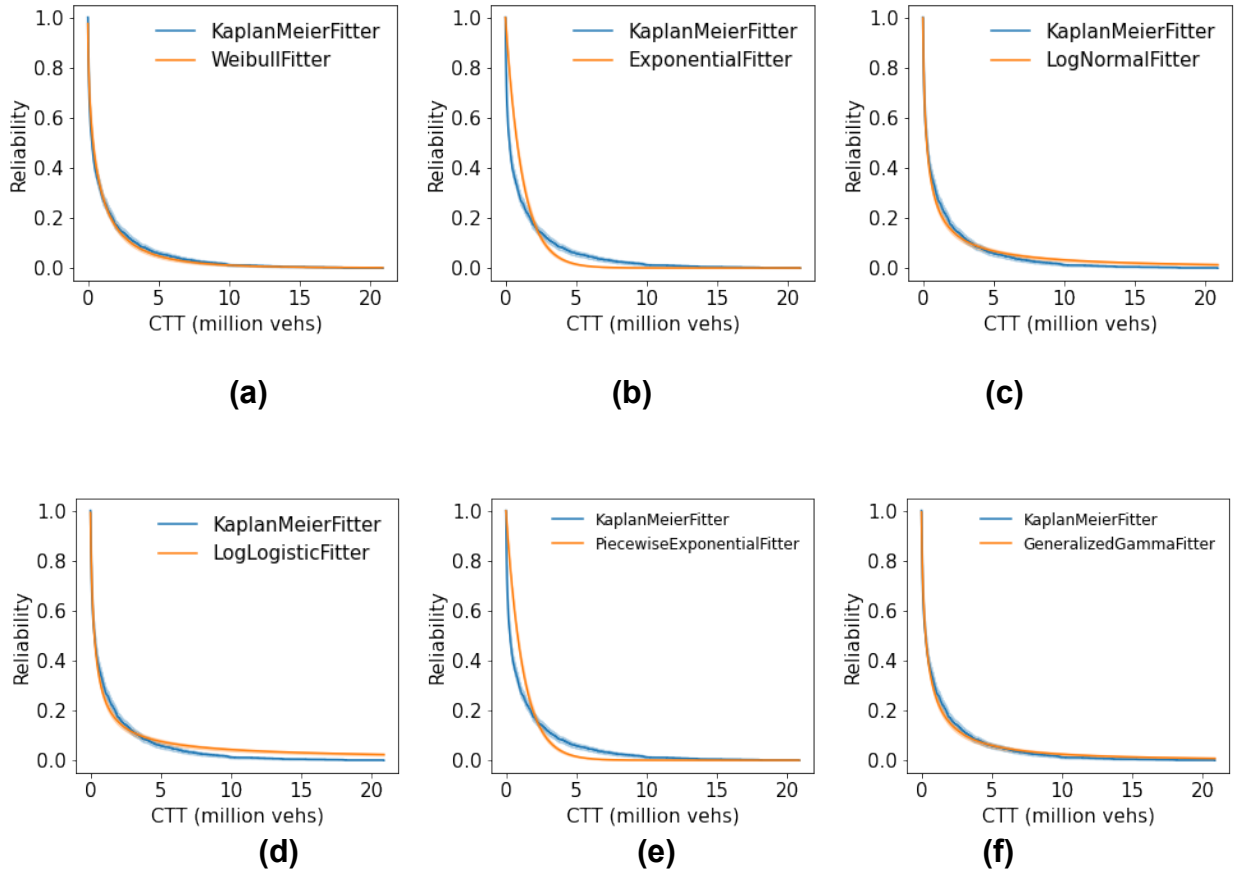

Figure 10. Estimated reliability curves of different distributions compared to the real deterioration pattern: (a) Weibull distribution, (b) exponential distribution, (c) log-normal distribution, (d) log-logistic distribution, (e) piecewise exponential distribution, and (f) generalized gamma distribution.

From Figure 10, it can be seen that Weibull distribution and generalized gamma distribution achieved better results compared to other distributions. The relative errors are as follows:

a) Weibull distribution: 4.0%
b) Exponential distribution: 49.7%
c) Log-normal distribution: 13.2%
d) Log-logistic distribution: 14.3%
e) Piecewise exponential distribution: 49.8%
f) Generalized gamma distribution: 8.7%

Looking at these results, it can be seen that the Weibull distribution can predict the reliability of bridge decks (i.e., the probability that a bridge will decrease in CR given the number of days it has already been at that rating) with the lowest relative error.

CHAPTER 5

Findings of the Weibull Deterioration Model

The Weibull deterioration model was then used to evaluate the deterioration at individual CRs (see Figure 11). The results show that bridge decks in good condition (e.g., CR9 and CR8) quickly deteriorate to a lower CR. As the CR decreases, such as CR7, CR6, and CR5, bridge decks spend a longer time at that CR. These bridge decks have the most reliable CRs with the slowest deterioration. However, at CR 4 bridge decks become unreliable again and the sojourn times decrease. These results suggest that the best time to perform bridge rehabilitation or maintenance is before the bridge deteriorates to a poor condition to avoid the unreliable CR 4.

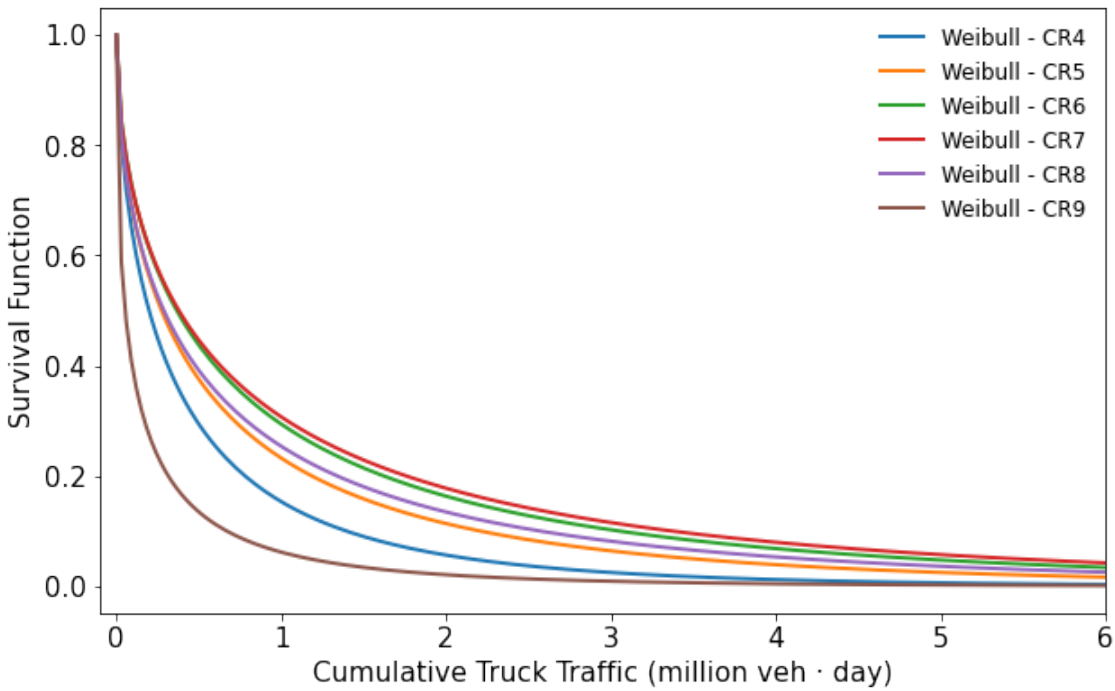

Figure 11. Prediction of Weibull model for each condition rating.

The Weibull distribution was then used to develop deterioration models for individual significant attributes for all condition ratings. Eleven models were developed for the bridge deck rebar type, main bridge spans, wearing surface type, and year built at each condition rating, and 6 condition ratings (i.e., CR 4 - CR 9) are modeled in this way. In total 66 models were developed for bridges with different attribute values at different condition ratings. The parameter estimation results of the different models for CR 7 are shown in Table 3. From Table 3, it can be observed that the standard error of each parameter is small and the p-value is ~0, which implies that the model achieved good performance.

Table 3. Model parameter estimation results of CR 7.

Attribute Values	μ	Standard Error of μ	P-Value of μ	σ	Standard Error of σ	P-Value of σ
Bridge Deck Rebar Type						
Bare Rebar	0.77	0.04	0.00	0.59	0.01	0.00
Galvanized Rebar	1.74	0.51	0.15	0.66	0.10	0.00
Epoxy Rebar	1.07	0.09	0.42	0.60	0.02	0.00
Main Bridge Spans (Number of Spans in Main Unit)						
Single Span	0.46	0.03	0.00	0.57	0.01	0.00
Multi-Span	1.19	0.07	0.01	0.61	0.02	0.00
Wearing Surface Types on the Bridge Main Span						
Concrete	0.68	0.05	0.00	0.55	0.02	0.00
Bituminous	0.47	0.03	0.00	0.60	0.01	0.00
Epoxy Overlay	2.39	0.49	0.00	0.71	0.08	0.00
Year Built						
Before1943	0.35	0.03	0.00	0.64	0.02	0.00
1943-1980	0.92	0.05	0.10	0.56	0.01	0.00
Post 1980	0.72	0.08	0.00	0.61	0.03	0.00

The deterioration of the bridge can then be calculated for a combination of attributes based on the weights as shown in Table 4 (note that the weights are used as an example to illustrate the approach and are not suggested weights).

Table 4. Combined prediction of deterioration probability of the bridge.

Attribute	Value	CR	Sojourn Time	Average Daily Truck Traffic	Cumu-lative Truck Traffic	Deterior-ation Probability	Weight	Overall Deterior-ation Probability
Rebar Type	Galvanized	7	2,000 (days)	1,000 (vehs/ day)	2 (million vehs)	0.70	1	0.81
Span Number	Single Span					0.89	1	
Surface Type	Asphalt					0.79	1	
Year Constructed	1990					0.86	1	

From Table 4, it can be seen that different attributes contribute to the deterioration probability independently, hence, the weighting factors play a large role in determining the final deterioration of the bridge. In fact, when the weight factors change, the deterioration of the bridge varies correspondingly. Figure 12 shows the change in overall deterioration of the bridge when the weight factors for different attributes vary from 0.1 to 2.0, keeping all other weight factors at 1. It can be seen that for this example,

increasing the weight of the rebar type or surface type decreases the overall deterioration probability, whereas increasing the weight of the span number or the year constructed increases the overall deterioration of the bridge. Also, the overall deterioration of the bridge is bounded by the minimum and maximum deterioration probability observed from the individual attributes. Note that these trends will be different when determining the overall deterioration of different bridges.

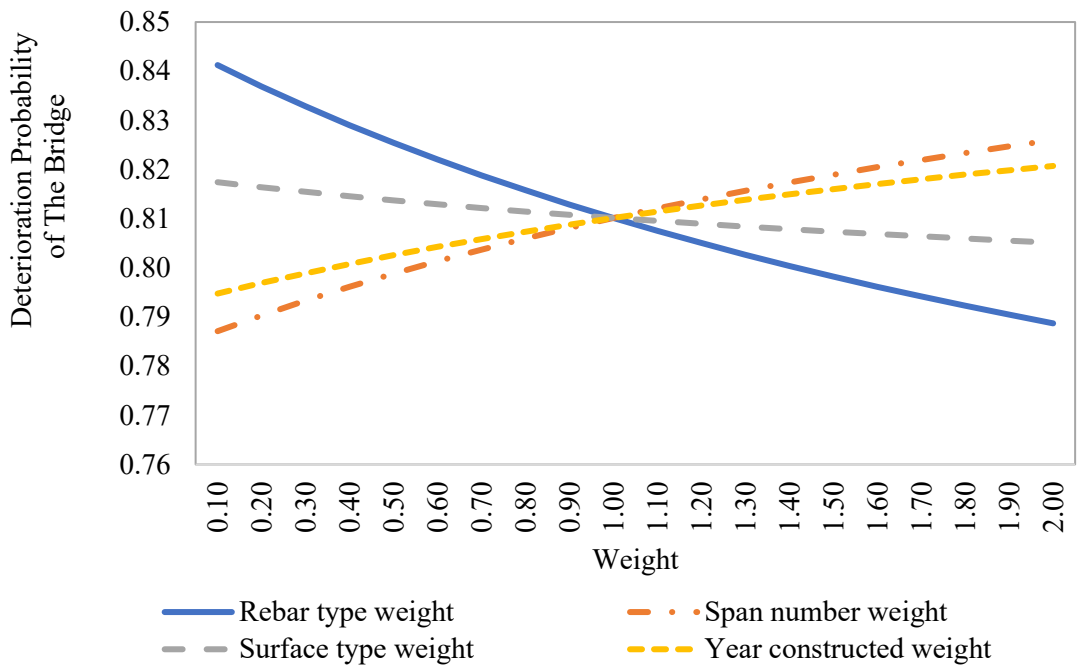

Figure 12. Sensitivity analysis of weights of different attributes.

CHAPTER 6

Findings of the Accelerated-failure Time Model

To obtain results using the proposed methodology, first the appropriate dependent variable using the available data was determined. Next, the fit of a generalized gamma distribution was compared to other possible distributions to verify that the proposed methodology fits the data best. To do so, only one variable, specifically the rebar type was considered, and the accuracy of the predictive model was analyzed. Next, all the attributes that are significant in predicting sojourn times were added to the model, and the influence of different attributes on the deterioration pattern were analyzed. Finally, the applicability of the Bayesian updating method was demonstrated. These steps are discussed in four consecutive subsections.

CHOOSING THE DEPENDENT VARIABLE

There were two candidates for choosing the dependent variable: (1) the time until the CR changes or (2) the total vehicle loading until the CR changes, or the cumulative truck traffic (CTT). Both of these variables could predict deterioration of bridge decks. However, since the purpose of this study was to analyze the reliability of bridges considering different attributes, time may not accurately reflect the reliability. In practice, the materials selections for bridge construction and repairs are often determined considering verity of factors, for example, average daily truck traffic. Consider the deck surface type as an example. Looking at the data, while 55.1% of bridges with ADTT less than 1,000 vehicles per day used the bituminous surface type, only 23.8% of bridges with ADTT larger than 1,000 vehicles per day used bituminous and instead 65.5% of them used a concrete surface. Hence, the average time until a change in CR of bridges with bituminous surface is larger than that for epoxy overlay and bituminous, as shown in Figure 13, even though this might not be due to the type of surface material (Michelle, 2018).

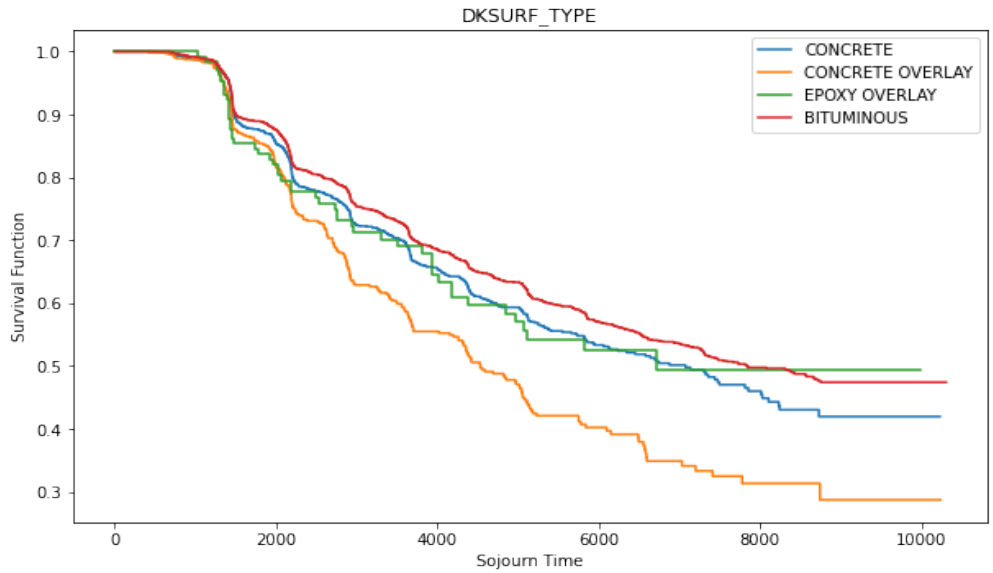

Figure 13. Deterioration pattern with time until change in CR as the independent variable.

To correct this deviation, the CTT was calculated by multiplying the time until a change in the CR and the average daily truck traffic to reflect the cumulative traffic loading on the bridge. The survival probability calculated according to the CTT is shown in Figure 14. From Figure 14, it can be observed that an epoxy overlay has the highest reliability, followed by the concrete overlay, and the bituminous has the lowest reliability for the same CTT.

Hence, the CTT was chosen as the dependent variable for this study. The models to analyze the deterioration pattern of a bridge deck were built to predict the survival probability given the CTT, which will be referred to as the sojourn time for the remainder of the report.

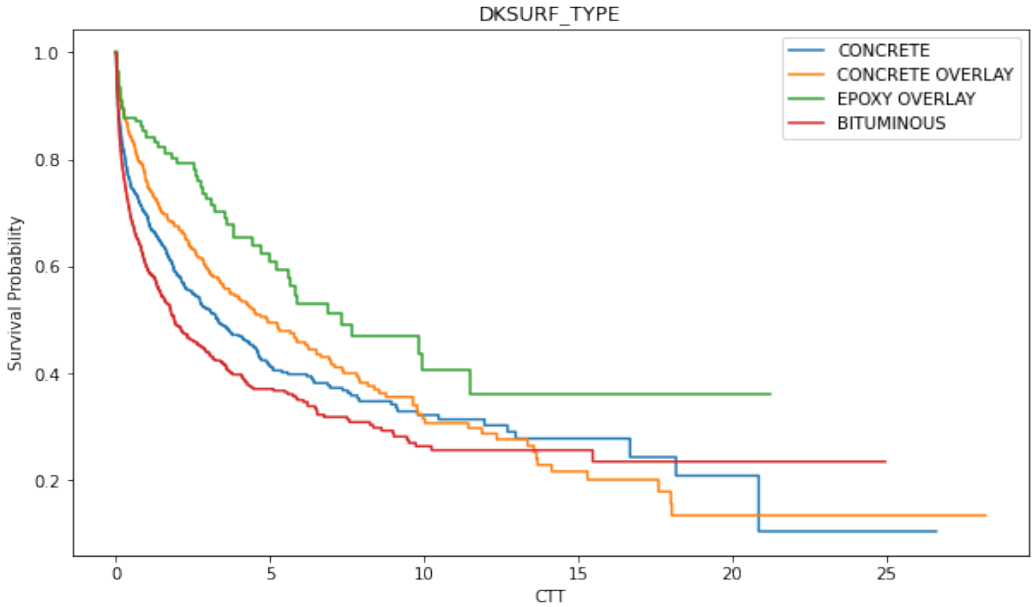

Figure 14. Deterioration pattern with CTT as the independent variable.

VERIFYING THE CHOICE OF GENERALIZED GAMMA DISTRIBUTION

Eight of the most popular distributions, exponential, Weibull, Gompertz, gamma, generalized gamma, log-normal, log-logistic and F, were chosen to compare the fit of the bridge deterioration inspection dataset used in this study. The non-parametric Kaplan-Meier reliability and the estimated parametric reliability for the six different distributions are shown in Figure 15, along with the relative error in the prediction of each distribution. Based on the results shown in Figure15 the best fit is achieved by the GGD model due to its flexibility. Hence, the analysis was continued with the GGD distribution.

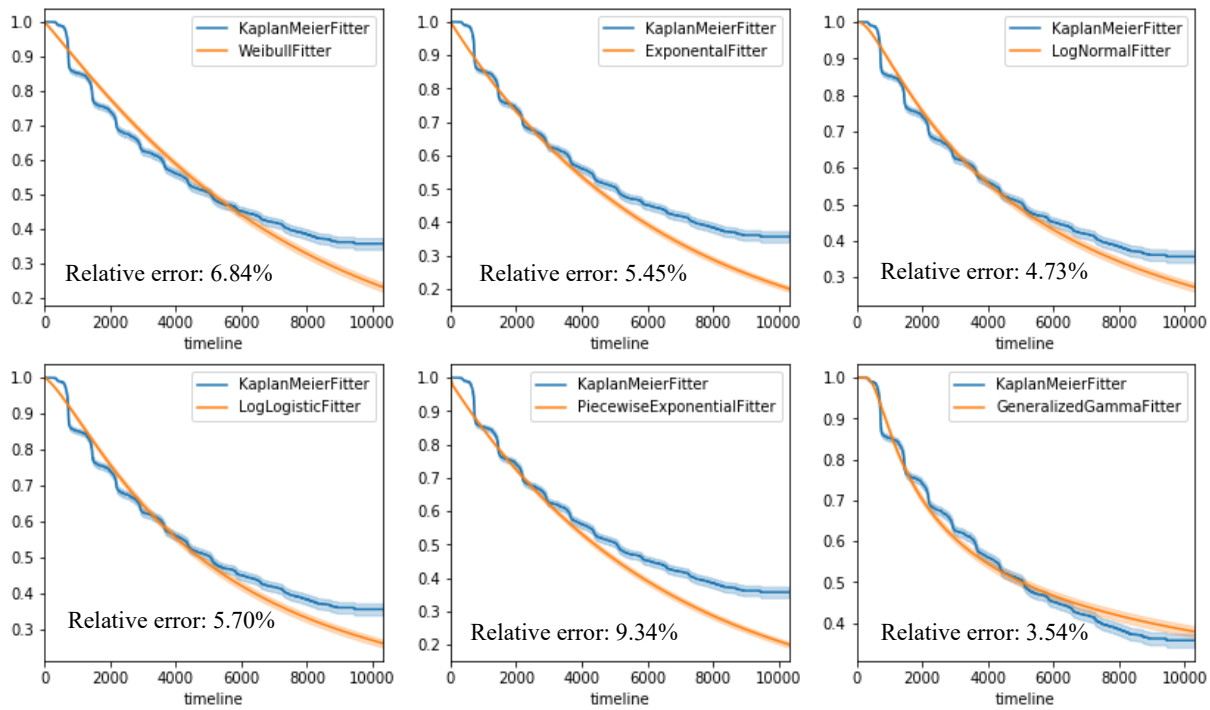

Figure 15. Results of different distributions used to model bridge survival probability function.

VERIFYING THE ACCURACY OF THE MCMC METHODOLOGY

To understand the appropriateness and accuracy of the MCMC methodology, first a model with only one predictor variable—rebar type—was estimated. To do so, the change in sojourn time as a function of the three major rebar types in the inspection data—bare rebar type, epoxy rebar type, and galvanized rebar type—was determined. A baseline that consists of all other rebar types was established.

3

The model parameters were estimated using: (1) a maximum likelihood estimation utilizing the Newton method (Peng, 2020), which is one of the most commonly used parameter estimation methods in the literature ; and (2) the Metropolis-Hasting MCMC method using 20,000 samples generated from the posterior distribution. Since the MCMC method provides a distribution for each parameter, the average parameter from this method was then estimated using either a Maximum A Posterior estimation (MAP) or simple mean. The resulting estimates can be seen in Figure 16 as the distribution of the parameter for the bare rebar, a normal distribution fitted to the parameter distribution, and the three point-estimates of the parameter.

From Figure 16, it can be observed that the three different point-estimates of the parameter are very similar. This indicates that the MCMC method can closely predict the parameter values compared to standard methods. The advantage of the MCMC method is that along with the point estimate it provides a distribution for the parameter, which can be used to determine bands of confidence around predictions of sojourn times and is also useful for updating the parameters as new data become available.

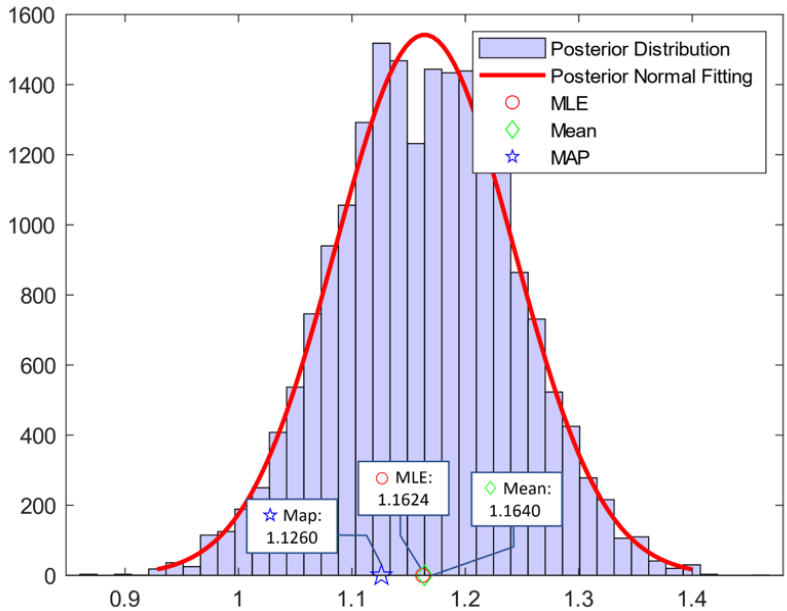

Figure 16. Comparison of estimation results of bared rebar type.

Since the samples can be closely fitted to a normal distribution, the MAP estimation and mean of sample should theoretically be identical. For the remainder of the report, the mean of the sample distribution is used as the point estimation for each parameter. Survival probability was determined using both the predictive model and Kaplan-Meier estimation, see Figure 17.

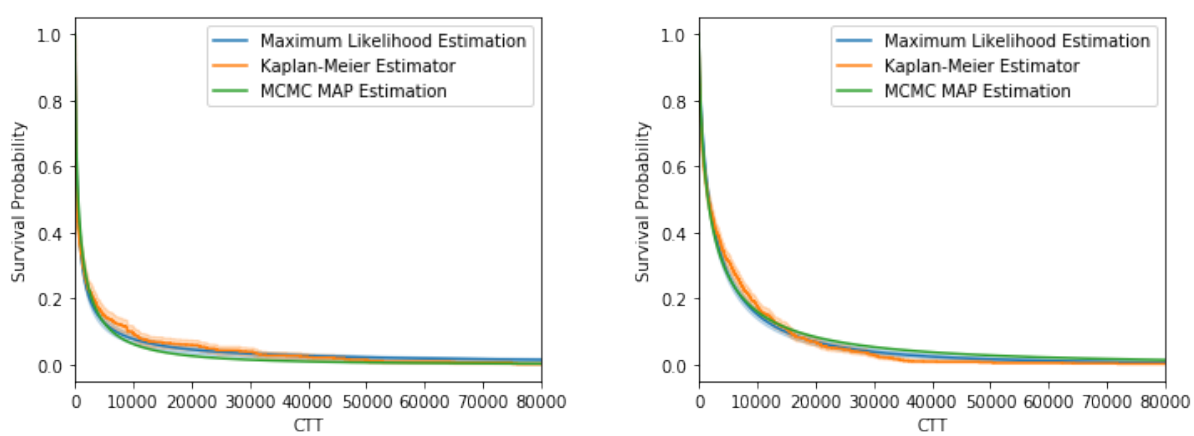

(a) (b)

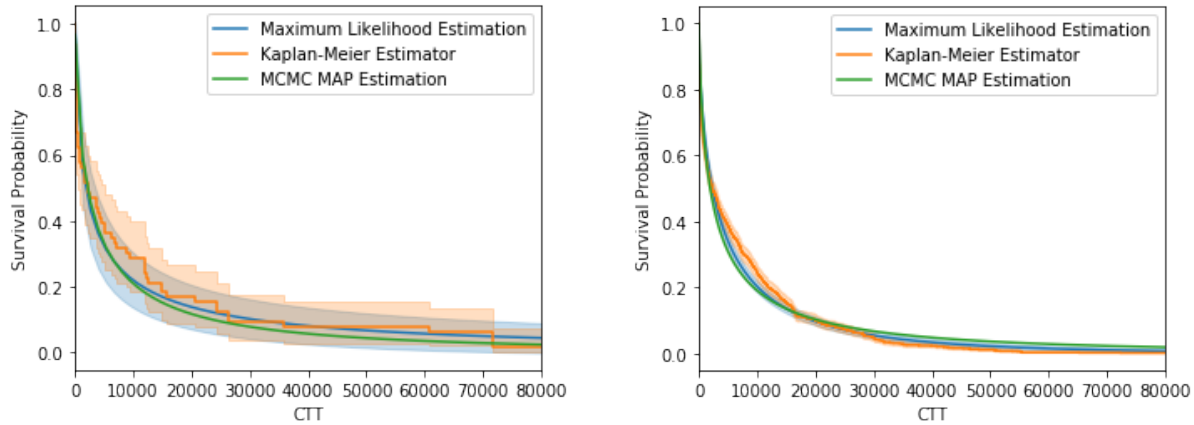

(c) (d)

Figure 17. Comparison of MCMC results and Kaplan-Meier estimation: (a) bare rebar, (b) galvanized rebar, (c) epoxy rebar, and (d) other rebar types (baseline).

From Figure 17, it can be seen that the predictive model has a high accuracy, can closely predict the deterioration pattern of different rebar types, and can distinguish the influence of different rebar types. A confusion matrix, which shows the accuracy of predicting the sojourn time using different rebar type variables, is calculated as shown in Table 5. For example, if the deterioration of a bridge deck with galvanized rebar is being predicted, however the model for bare rebar was used, the relative error would be 0.33. It can be seen that the model has the largest accuracy along the diagonal, which is when the correct rebar type from the data is used to predict the sojourn time of the data.

Table 5. Confusion matrix of the predictive model.

Relative Error		Real Data Bare Rebar	Real Data Galvanized Rebar	Real Data Epoxy Rebar	Real Data Rebar Baseline
Predicted Data	Bare Rebar	**0.15**	0.46	0.33	0.48
	Galvanized Rebar	0.33	**0.16**	0.22	0.70
	Epoxy Rebar	0.16	0.18	**0.14**	0.59
	Rebar Baseline	0.64	1.11	0.93	**0.31**

ESTIMATION OF THE FULL MODEL

Next, a full model considering all attributes for CR 4 through CR 9 was estimated. To do so, all data were initially included in the model and backward elimination was performed. Finally, 41 attributes were included for various CR ratings. Using these attributes, 20,000 samples of the MCMC were generated, and the mean of the coefficients estimated is shown in Table 6. Notice that each discrete variables' coefficient was estimated considering a baseline, and not all attributes were significant for different CR values. If a level of a discrete variable was not significant, it was included in the baseline (e.g., District 2 and District 8 make up the baseline for CR 4).

Table 6. Estimated parameters of the full model.

Attributes	CR 4	CR 5	CR 6	CR 7	CR 8	CR9
District						
District 1	-0.172	-0.1381	-0.2728	-0.5901	-0.0894	0.0162
District 2	*	-0.0997	*	-0.7327	*	0.327
District 3	-0.4446	-0.4267	-0.1247	-0.4232	*	-0.2198
District 4	0.7709	*	0.0649	-0.4061	0.506	-0.0398
District 5	1.0466	0.598	0.4514	*	1.1258	0.7528
District 6	0.0359	0.9389	0.8934	0.641	1.2452	0.8245
District 8	*	0.1756	*	*	0.5437	0.4424
District 9	-0.2991	*	-0.3522	-0.6383	-0.2432	-0.5398
District 10	-0.4664	-0.4978	*	-0.7578	-0.0016	-0.4088
District 11	0.3295	*	0.3404	0.2328	0.6338	*
District 12	0.1242	*	-0.3278	-0.7794	0.338	*
Main Materials Type						
Steel	*	*	*	*	*	-0.3919
Concrete (Cast in Place)	0.2031	-0.2634	-0.267	0.678	0.3162	*
Concrete (Precast)	-	-0.5625	-0.4967	0.4	-0.3127	-
Prestressed Precast Concrete	*	*	*	*	-0.1634	-0.7049
Concrete Encased Steel	0.1904	0.4508	0.1754	0.4344	0.1246	-
Physical Makeup of the Main Span of the Structure						
Reinforced	0.4344	1.4082	0.9421	0.3849	0.3278	*
Pretensioned	*	*	*	*	*	0.5282
Rolled Sections	-0.1781	*	-0.2153	-0.1943	-0.0124	0.5223
Rolled Sections with Cover Plates	-0.6588	*	-0.3695	-0.4118	-0.5	-
Combo, Rolled Sections/Cover-Plates	-	0.2895	-0.1294	-0.578	-	-
Other	0.2566	*	-0.1561	-0.1998	0.11	0.0811
Span Interaction for the Main Span of the Structure						
Simple, Non-Composite	-0.0664	-0.1583	-0.3387	-0.1015	-0.2207	-0.184
Continuous, Non-Composite	-0.3865	0.089	-0.1764	0.2442	0.4293	-
Continuous, Composite	0.1907	-0.0733	0.2347	0.3572	0.0206	-0.32
Other	0.1987	-0.2811	-0.243	-0.1141	-0.4062	-
Structural Configuration for the Main Span of the Structure						
Slab (Solid)	-0.7481	-0.9218	-0.8948	-0.9919	-0.4654	0.1931
T-Beams	-0.2448	-0.5426	-0.3899	-0.848	-0.247	0.8732
I Beams	*	*	*	*	0.1833	*
Box Beam - Single	-0.2722	-0.2242	-0.4843	-0.5586	*	0.2272
Box Beam - Adj	-0.4231	-0.485	-0.6576	-0.6051	-0.3807	-0.2772
I-Welded Beams	-	-1.1168	-0.538	-0.7838	-0.2569	-
Girder Weld/Deck	-0.5607	0.1753	0.2236	-0.0005	*	-
Truss - Deck	-	-	-	1.2577	-	-
Rigid Frame	-	-1.9073	-0.8808	-1.0065	-	-
Deck Protection Type						
Epoxy Coated Reinforcing	*	*	*	0.4535	0.4208	0.2034
Galvanized Reinforcing	-	-0.0321	*	0.8791	0.6218	-
Deck Rebar Type						
Epoxy Rebar	0.464	0.4066	0.3161	-	0.0724	0.5141
Galvanized Rebar	*	0.2146	-0.0435	-0.6243	-0.233	*
Others	-0.311	-	-0.2592	-0.3624	-0.1209	-0.1343

Attributes	CR 4	CR 5	CR 6	CR 7	CR 8	CR9
Main Bridge Spans (Number of Spans in Main Unit)						
1	*	*	0.1717	0.2323	*	*
2	-0.0423	-0.2493	*	*	-0.1913	0.2646
3	0.9023	0.7065	0.9246	0.7042	0.4596	0.8411
4	0.1244	-0.2311	*	0.1665	0.1174	-0.0462
5	1.224	0.3203	0.295	*	0.0645	-
6	-	-	0.0878	-0.2673	-	-
Waterproofing Membrane on the Bridge Main Span						
Preformed Fabric	0.0913	0.558	*	0.2054	0.406	0.5369
Epoxy	-	-	-	-0.0879	-	-
Other	-	-0.3782	-0.7985	-0.8029	-	-
Wearing Surface Types on the Bridge Main Span						
Concrete Overlay	0.462	0.6124	0.6774	0.5288	0.6413	0.5869
Epoxy Overlay	0.7728	0.9731	0.7558	0.8091	1.0521	-
Bituminous	0.4119	*	0.4016	0.4239	0.4598	0.5825
Special Events						
Sharply Decrease	-0.9948	-0.8328	-0.4298	-0.403	-0.6643	*
Nothing Happened	*	*	*	*	0.5094	2.803
Sharply Increase	*	-0.293	-0.2683	-0.4494	*	*
Length	0.1736	0.3423	0.3293	0.4505	0.1212	0.653
Deck Width	10.2289	9.5222	8.4817	10.4584	10.5333	11.322
Ln (Sigma)	0.4118	0.4726	0.4288	0.4351	0.3678	0.4232
Lambda	0.6226	0.3328	0.4375	0.4071	0.3318	0.2827
Beta_0	-3.6452	-4.2849	-3.9917	-4.4316	-6.2533	-7.4602

Note: "-" means a baseline of each model, which has a similar deterioration pattern with the full dataset; "*" means that not enough data were available for such attribute type to feed the model (denotes less than 500).

From Table 6, it can be seen that the influence of each attribute for different condition ratings varies slightly; however, the trends are consistent. Some detailed results and observations from Table 6 are discussed below.

The mean value of the parameters of the DISTRICT attribute for each CR is plotted in Figure 18, along with the error bars that represent the standard deviations of those samples. Bridges from different districts have different management strategies, environmental conditions, budgets, and traffic conditions, hence bridge performance varies among districts. Bridges that have the highest reliability are in districts 5 and 6, which are located in eastern Pennsylvania, which is most likely due to economic development and weather conditions in that location.

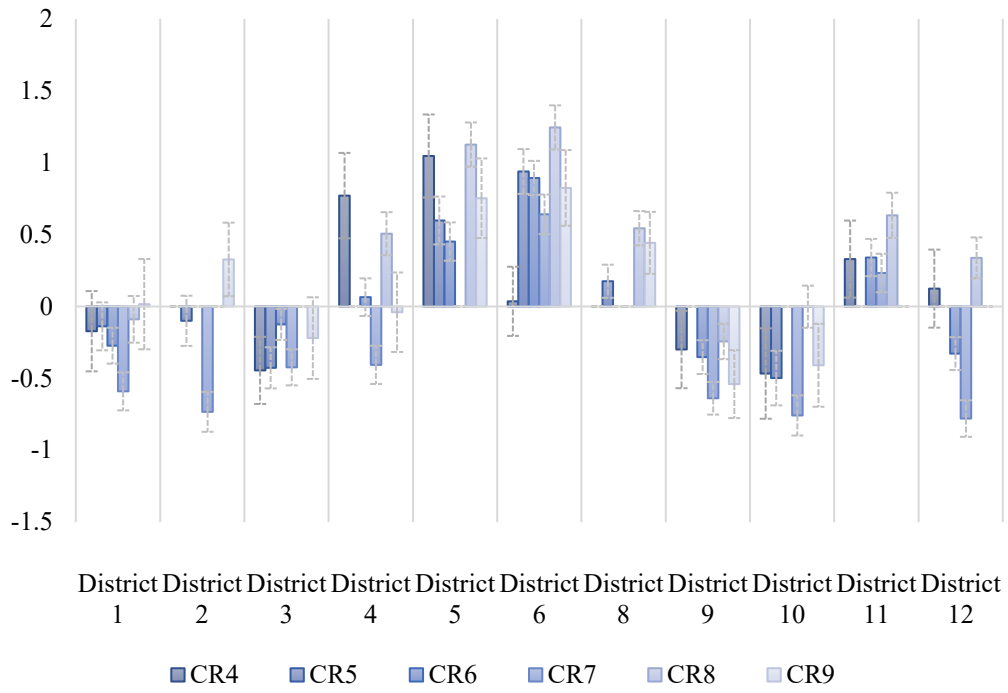

Figure 18. Parameters of DISTRICT in each condition rating.

The DEPT_MAIN_PHYSICAL_TYPE attribute denotes the physical makeup of the main span of the structure. Figure 19 shows the reliability parameters of different physical makeup types. The reinforced type has the highest reliability compared to the other types. From Table 6, it can be seen that the pretensioned type is mostly chosen as a baseline, which implies that the reliability of the pretensioned type is between the reinforced type and the rolled sections with cover plates.

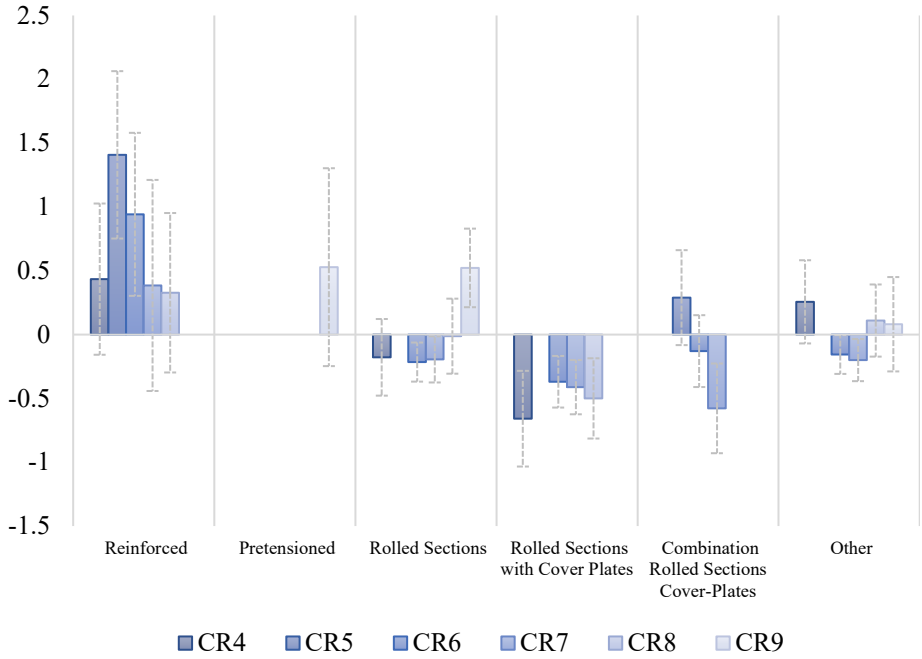

Figure 19. Parameters of DEPT_MAIN_PHYSICAL_TYPE in each condition rating.

Figure 20 shows that continuous span interactions for the main span of the structure are generally the strongest as compared to simple spans and others, and composite is slightly better that noncomposite in most condition ratings (i.e., CR 4, CR 6, CR 7).

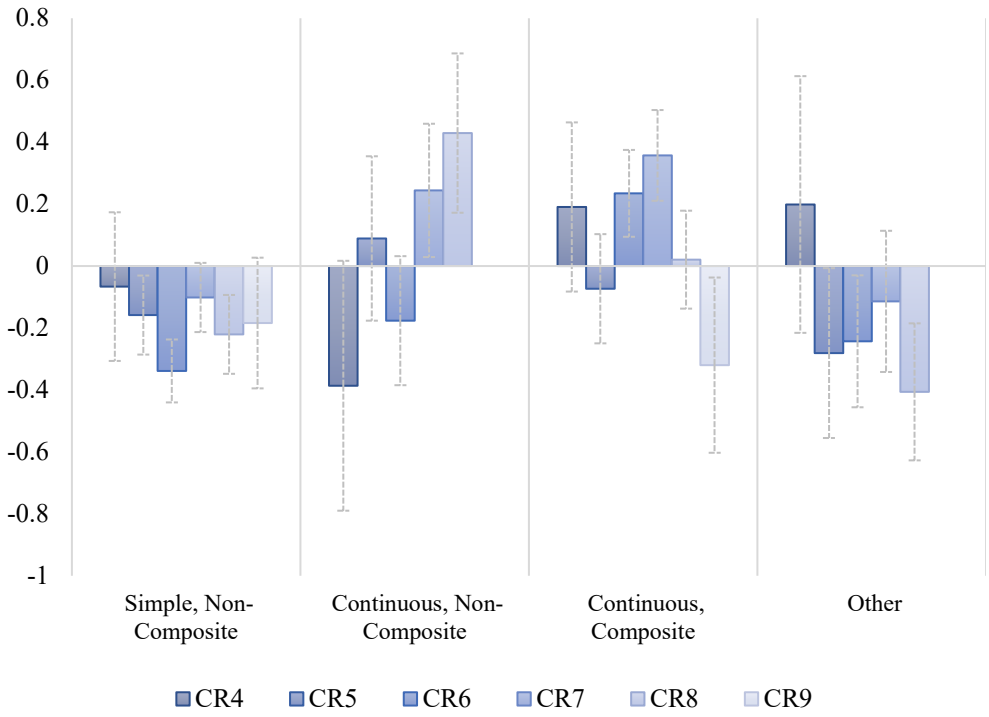

Figure 20. Parameters of DEPT_MAIN_SPAN_INTERACTION in each condition rating.

The results of DECK_REBAR_TYPE show that galvanized rebar and epoxy rebar performs better than others, and epoxy rebar is slightly better than galvanized rebar. However, due to the few data of epoxy rebar, the confidence interval of the parameters of epoxy rebar is large, see Figure 21.

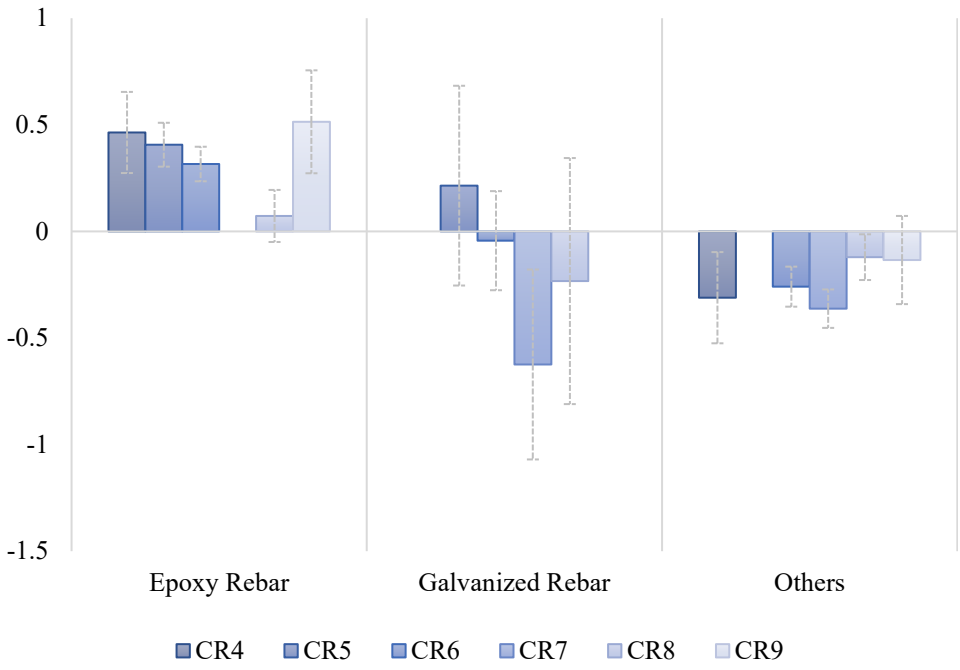

Figure 21. Parameters of DECK_REBAR_TYPE in each condition rating.

Another interesting result is obtained for bridge decks that experience sharp (more than two condition ratings between two consecutive inspections) declines or increases in condition ratings. The sudden increases could be due to a maintenance or reconstruction activity, and the sudden declines could be due to an incident happening on the bridge causing it to deteriorate quickly in a short time. Figure 22 shows the parameters for the baseline (i.e., only smooth transitions, type 1: sudden increase, and type 2: sudden decrease). The model results show that after a bridge has been maintained, the condition of the bridge will not have the same performance as a bridge at the same condition rating that was not reconstructed. Every time when the bridge has been maintained, the reliability will drop slightly as compared to a newly constructed bridge. On the other hand, comparing type 1 to type 2, it can be seen that damage to a bridge has a larger impact on the reliability of the bridge as compared to a controlled maintenance activity being performed.

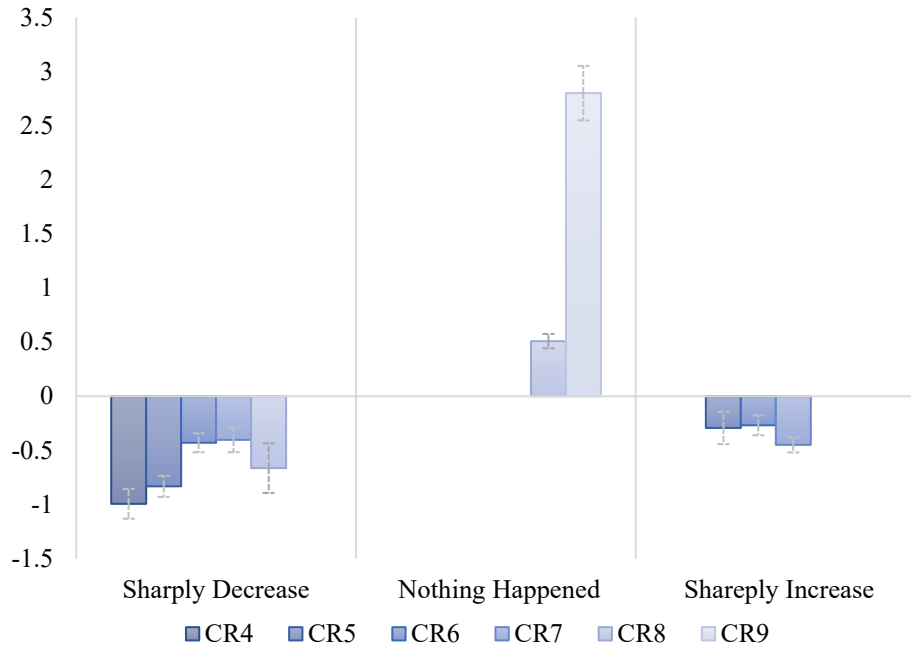

Figure 22. Parameters of SPECIAL EVENTS in each condition rating.

Additionally, since all the attributes were incorporated into the model as a binary variable (0 or 1), and the coefficient of a given attribute represents the independent influence of this attribute, the model can easily be used to understand the reliability of bridges considering multiple attributes by simply summing their coefficients. For example, when a new bridge with a bare rebar type is constructed in district 2, and another with a galvanized rebar type is built in district 5, the reliability of the two bridges can be directly compared by adding the coefficients of the relevant rebar type and district number from the model to obtain the reliability of each bridge. This feature can be used in analyzing the reliability of newly constructed bridges.

Bayesian Estimation Results

As new inspection data become available, the old model will require updating. In this case, Bayesian theory can be utilized to update the parameters of the existing model. The CR 6 dataset was utilized to demonstrate the proposed method.

Firstly, the dataset was divided into two parts according to the inspection date of the bridge. The first dataset consisted of all the inspection data before 2000, and the second dataset consisted of all the inspection data between 2000 and 2015. Another test that used the entire dataset as one was also developed to compare to the two-step updated results. The number of observations that were available in each dataset are shown in Table 7.

Table 7. Dataset description.

Dataset	Censored Data	Complete Data	Total
1985-2000	5,404	1,301	6,705
2000-5015	5,405	2,470	7,875
1985-2015 (Entire dataset)	7,264	3,827	11,091

First, dataset 1 was modeled as described using a beta distribution as the prior distribution and using the MCMC method; 20,000 samples were generated from the posterior distribution. A normal distribution was used to fit these samples to obtain the posterior distribution (see Step 1, blue histograms and fitted curves in Figure 23). Next, the fitted normal distributions for each parameter were used as the prior distribution for determining the posterior distribution using dataset 2. Again, 20,000 samples were generated from the posterior distribution and a normal distribution was used to fit the samples to obtain the posterior distribution (see Step 2, yellow histograms and fitted curves in Figure 23). The results from the test using the entire, complete dataset at once are also shown below (see all data, red histograms and fitted curves in Figure 23) to compare the results from the updating process and direct calculation.

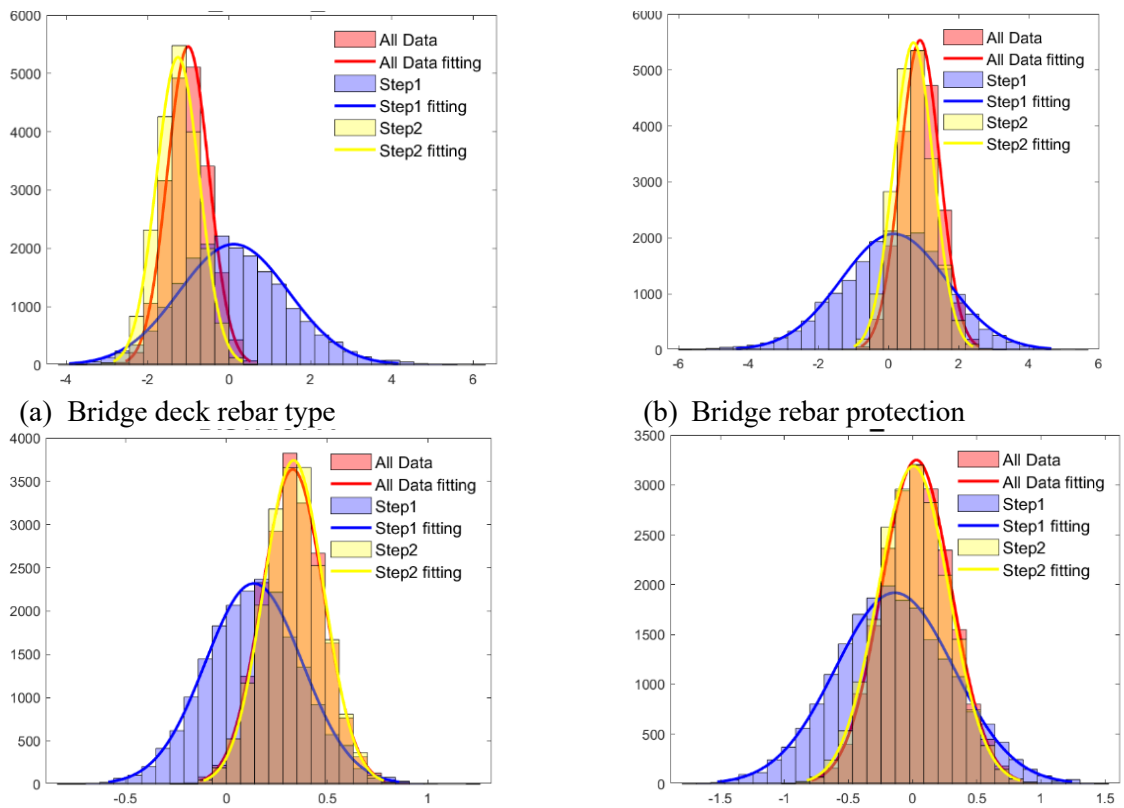

(a) Bridge deck rebar type

(b) Bridge rebar protection

(c) District

(d) Number of main spans

Figure 23. Bayesian updating results.

From Figure 23, it can be observed that as more data become available, the samples become more concentrated, and the accuracy of the predictive model is improved. The interval estimation also resulted in a narrower range. The updated results are very similar to the direct calculations, which showed that the Bayesian updating method can obtain reliable results.

CHAPTER 7

Recommendations

Condition ratings from inspection points of 22,000 bridges in Pennsylvania were collected over a 30-year span. Bridges in Pennsylvania experience a skewed right distribution and will stay at a condition rating for an average of 2,849 days (7.7 years) and a standard deviation of 1,621 days (4.4 years). Bridge attributes were compared to see how different attributes and truck traffic influence the deterioration rate of a bridge. Based on the data provided by PennDOT, the epoxy rebar and galvanized rebar show a higher reliability compared to the bare rebar, and the single-span bridges can take heavier traffic loads than multi-span bridges. The epoxy overlay is stronger than concrete or asphalt surface when the bridge is in good condition, but its reliability will drop more quickly once the bridge deteriorates to the lower condition rating due to cracks. Similarly, asphalt overlays are particularly useful when the bridge is already in good condition; however, the difference between asphalt overlays and others is more negligible as deterioration sets in. It was also found that the bridges constructed between 1943 and 1980 suffer higher truck traffic but still, with the similar sojourn times, this indicated that the bridges constructed between 1943 and 1980 have a higher reliability compared to others.

Furthermore, a new perspective on analyzing the influence of different attributes of bridge decks on the deterioration process is examined. Instead of the traditional approach that considers the influence of attributes on the bridge's reliability for different times, the authors found that it is more reasonable to analyze this impact from the view of the cumulative truck traffic. Consequently, the reliability of the bridge can be more accurately related to the attributes and it is possible to quantify the influence of different attributes on bridge deck reliability.

It was also found that a generalized gamma distribution is more suitable to model the bridge deck deterioration pattern, compared to other commonly used distributions, such as Weibull distribution, log-normal distribution, and gamma distribution. The accelerated failure time approach was also implemented in this model to incorporate the attributes of bridge decks. A parameter estimate approach was designed for the AFT-GGD model, which overcomes the convergence problem and computational problems during programing.

In order to realize the self-updating function to make the model more flexible and efficient, Bayesian inference was used to update each parameter when new data become available. The MCMC method was utilized to obtain the full posterior distribution of parameters based on Bayesian theory. A case study showed that the proposed method in this study had high accuracy and efficiency of updating.

The model results provided a quantitative comparison of reliabilities of bridges with different attributes and the deterioration probability can be calculated under specific conditions. The district where bridges are located, the rebar type, the surface overlay type, as well as other attributes have a significant influence on the bridge deterioration process. By using the proposed model, the reliability of new bridges can be calculated, and the model can be updated as new inspection data come in real time.

References

Agrawal, A.K., Kawaguchi, A., and Chen, Z., 2010a. Deterioration Rates of Typical Bridge Elements in New York. *Journal of Bridge Engineering* 15, 419–429. https://doi.org/10.1061/(ASCE)BE.1943-5592.0000123

Bayes, C.L., and Branco, M.D., 2007. Bayesian inference for the skewness parameter of the scalar skew-normal distribution. *Brazilian Journal of Probability and Statistics* 21, 141–163.

Bektaş, B.A., 2017. Use of Recursive Partitioning to Predict National Bridge Inventory Condition Ratings from National Bridge Elements Condition Data. *Transportation Research Record* 2612, 29–38. https://doi.org/10.3141/2612-04

Belitser, E., and Ghosal, S., 2003. Adaptive Bayesian inference on the mean of an infinite-dimensional normal distribution. *Ann. Statist*. 31, 536–559. https://doi.org/10.1214/aos/1051027880

Bu, G.P., Lee, J.H., Guan, H., Loo, Y.C., and Blumenstein, M., 2015. Prediction of Long-Term Bridge Performance: Integrated Deterioration Approach with Case Studies. *Journal of Performance of Constructed Facilities* 29, 04014089. https://doi.org/10.1061/(ASCE)CF.1943-5509.0000591

Contreras-Nieto, C., Shan, Y., and Lewis, P., 2018. Characterization of Steel Bridge Superstructure Deterioration through Data Mining Techniques. *Journal of Performance of Constructed Facilities* 32, 04018062. https://doi.org/10.1061/(ASCE)CF.1943-5509.0001205

Cox, C., and Matheson, M., 2014. A Comparison of the Generalized Gamma and Exponentiated Weibull Distributions. *Stat Med* 33, 3772–3780. https://doi.org/10.1002/sim.6159

de Pascoa, M.A.R., Ortega, E.M.M., and Cordeiro, G.M., 2011. The Kumaraswamy generalized gamma distribution with application in survival analysis. *Statistical Methodology* 8, 411–433. https://doi.org/10.1016/j.stamet.2011.04.001

Enrique de Alba ASA, P., 2006. Claims Reserving When There Are Negative Values in the Runoff Triangle. *North American Actuarial Journal* 10, 45–59. https://doi.org/10.1080/10920277.2006.10597402

Guler, S. I., and Madanat, S., 2011. Axle Load Power for Pavement Fatigue Cracking: Empirical Estimation and Policy Implications. *Transportation Research Record* 2225(1), 21–24. https://doi.org/10.3141/2225-03.

Huang, Y.-H., 2010. Artificial Neural Network Model of Bridge Deterioration. *Journal of Performance of Constructed Facilities* 24, 597–602. https://doi.org/10.1061/(ASCE)CF.1943-5509.0000124

Kaniovski, S., and Peneder, M., 2008. Determinants of firm survival: A duration analysis using the generalized gamma distribution. *Empirica* 35, 41–58. https://doi.org/10.1007/s10663-007-9050-3

Kaplan, E.L., and Meier, P., 1958. Nonparametric Estimation from Incomplete Observations. *Journal of the American Statistical Association* 53, 457–481. https://doi.org/10.2307/2281868

Lawless, J.F., 2011. *Statistical Models and Methods for Lifetime Data*. John Wiley & Sons.

Manafpour, A., Guler, I., Radlińska, A., Rajabipour, F., and Warn, G., 2018. Stochastic Analysis and Time-Based Modeling of Concrete Bridge Deck Deterioration. *Journal of Bridge Engineering* 23, 04018066. https://doi.org/10.1061/(ASCE)BE.1943-5592.0001285

Michelle, U., 2018. What's the Difference? Concrete vs. Asphalt Driveways. Bob Vila. URL https://www.bobvila.com/articles/concrete-vs-asphalt-driveways/ (accessed 5.25.20).

O'Leary, N., Chauhan, B.C., and Artes, P.H., 2012. Visual Field Progression in Glaucoma: Estimating the Overall Significance of Deterioration with Permutation Analyses of Pointwise Linear Regression

(PoPLR). *Invest. Ophthalmol. Vis. Sci.* 53, 6776–6784. https://doi.org/10.1167/iovs.12-10049

Peng, R.D., 2020. *Advanced Statistical Computing*.

Pennsylvania Department of Transportation, 2009. "PUB 100A- Bridge Management System 2 Coding Manual." July 2009 Edition.

http://www.dot.state.pa.us/public/PubsForms/Publications/Pub_408/408_2020/408_2020_IE/408_2020_IE.pdf (accessed 2.3.20).

Pennsylvania Department of Transportation, 2020. "Pub 408 - Construction Specifications," https://www.penndot.gov:443/ProjectAndPrograms/Construction/Pages/ConstructionSpecifications.aspx (accessed May 19, 2020).

Pennsylvania Department of Transportation, 2020. Performance Results [WWW Document], n.d. URL https://www.penndot.gov/about-

Prozzi, J. A., and Madanat, S.M., 2000. Using Duration Models to Analyze Experimental Pavement Failure Data. *Transportation Research Record* 1699(1), 87–94. https://doi.org/10.3141/1699-12.

Strauss, A., Frangopol, D.M., Kim, S., 2008. Use of monitoring extreme data for the performance prediction of structures: Bayesian updating. *Engineering Structures* 30, 3654–3666. https://doi.org/10.1016/j.engstruct.2008.06.009

Tabatabai, H., Tabatabai, M., and Lee, C.-W. Lee, 2011. Reliability of Bridge Decks in Wisconsin. *Journal of Bridge Engineering* 16(1), 53–62. https://doi.org/10.1061/(ASCE)BE.1943-5592.0000133.

Yang, Y.-J., Wang, W., Zhang, X.-Y., Xiong, Y.-L., Wang, G.-H., 2018. Lifetime data modelling and reliability analysis based on modified Weibull extension distribution and Bayesian approach. *J Mech Sci Technol* 32, 5121–5126. https://doi.org/10.1007/s12206-018-1009-8

Zhang, W., and Durango-Cohen, P.L., 2014. Explaining Heterogeneity in Pavement Deterioration: Clusterwise Linear Regression Model. *Journal of Infrastructure Systems* 20, 04014005. https://doi.org/10.1061/(ASCE)IS.1943-555X.0000182